

# Altering the redox status of *Chlamydia trachomatis* directly impacts its developmental cycle progression

Reviewed Preprint

v1 • July 16, 2024

Not revised

Vandana Singh, Scot P Ouellette 

Department of Pathology, Microbiology, and Immunology, College of Medicine, University of Nebraska Medical Center, Omaha, NE 68198

 [https://en.wikipedia.org/wiki/Open\\_access](https://en.wikipedia.org/wiki/Open_access)
 Copyright information

## Abstract

*Chlamydia trachomatis* is an obligate intracellular bacterial pathogen with a unique developmental cycle. It differentiates between two functional and morphological forms: elementary body (EB) and reticulate body (RB). The signals that trigger differentiation from one form to the other are unknown. EBs and RBs have distinctive characteristics that distinguish them, including their size, infectivity, proteome, and transcriptome. Intriguingly, they also differ in their overall redox status as EBs are oxidized and RBs are reduced. We hypothesize that alterations in redox may serve as a trigger for secondary differentiation. To test this, we examined the function of the primary antioxidant enzyme alkyl hydroperoxide reductase subunit C (AhpC), a well-known member of the peroxiredoxins family, in chlamydial growth and development. Based on our hypothesis, we predicted that altering the expression of *ahpC* will modulate chlamydial redox status and trigger earlier or delayed secondary differentiation. To test this, we created *ahpC* overexpression and knockdown strains. During *ahpC* knockdown, ROS levels were elevated, and the bacteria were sensitive to a broad set of peroxide stresses. Interestingly, we observed increased expression of EB-associated genes and concurrent higher production of EBs at an earlier time in the developmental cycle, indicating earlier secondary differentiation occurs under elevated oxidation conditions. In contrast, overexpression of AhpC created a resistant phenotype against oxidizing agents and delayed secondary differentiation. Together, these results indicate that redox potential is a critical factor in developmental cycle progression. For the first time, our study provides a mechanism of chlamydial secondary differentiation dependent on redox status.

### eLife assessment

In this **valuable** study, the authors propose a model wherein the bacterial redox state plays a crucial role in the differentiation of *Chlamydia trachomatis* into elementary and reticulate bodies. They provide evidence to argue that a highly oxidising environment favours the formation of elementary bodies while a reducing condition slows down development. Whilst aspects related to the role of AhpC in regulating redox, and implications on differentiation, are **solid**, more precise measurements of the redox potential are required to **convincingly** demonstrate the role of redox in developmental progression.

<https://doi.org/10.7554/eLife.98409.1.sa3>

## Introduction

All organisms that are exposed to oxygen are necessarily subjected to oxidative stress. Specifically, the process of metabolizing substrates in the presence of oxygen can generate reactive oxygen species (ROS), which are toxic at high enough concentrations. Thus, from bacteria to humans, systems have evolved to mitigate the accumulation of ROS. At the same time, host defense mechanisms have evolved to leverage ROS production as a means of limiting pathogen growth and survival. Not surprisingly, pathogens have co-evolved to resist these defense mechanisms. For example, many pathogens possess a variety of antioxidant enzymes, such as catalases, glutathione peroxidases, and peroxiredoxins, that help them both subvert ROS-mediated immune system assaults and mitigate metabolic ROS byproducts (Staerck et al., 2017 [↗](#); Wan et al., 2021 [↗](#)).

*Chlamydia* is an obligate intracellular bacterium that has significantly reduced its genome size and content in adapting to obligate host dependence. *Chlamydia trachomatis*, the leading cause of bacterial sexually transmitted diseases and preventable infectious blindness, lacks homologs to catalases or glutathione peroxidases but does possess a homolog of Alkyl hydroperoxide reductase subunit C (AhpC). AhpC is a well-known member of the peroxiredoxins family and is widely conserved in prokaryotes (de Oliveira et al., 2021 [↗](#)). Peroxiredoxins can scavenge hydrogen peroxide, peroxynitrite, and organic hydroperoxides (Parsonage et al., 2008 [↗](#); Poole & Ellis, 1996 [↗](#); Seaver & Imlay, 2001 [↗](#)) and act as the primary scavenger in pathogens that lack both catalase and glutathione peroxidases (Mastronicola et al., 2014 [↗](#); Richard et al., 2011 [↗](#)). Several studies from other bacterial systems have shown that AhpC has a significant role in ROS and RNI scavenging, virulence, and persistence (Cosgrove et al., 2007 [↗](#); Kimura et al., 2012 [↗](#); Oh & Jeon, 2014 [↗](#)), and deletion of AhpC creates highly oxidized conditions within the bacterium (Zhang et al., 2019 [↗](#)). However, the function of AhpC in chlamydial biology has not been characterized.

*Chlamydia* is unique among pathogens in undergoing a complex developmental cycle that comprises two distinct morphological forms, the elementary body (EB) and reticulate body (RB) (Abdelrahman & Belland, 2005 [↗](#)). The EB is the smaller (~0.3 µm), infectious, and non-dividing form capable of infecting susceptible host cells. Once internalized into a host-derived vacuole termed an inclusion, the EB differentiates into the non-infectious, larger (~1 µm), and replicating RB - this process is known as primary differentiation and represents the early phase of the developmental cycle (Clifton et al., 2005 [↗](#)). RBs replicate within the inclusion in the mid-cycle phase using an asymmetric, MreB-dependent polarized division process (Abdelrahman et al., 2016 [↗](#); Lee et al., 2020 [↗](#); Ouellette et al., 2022 [↗](#); Ouellette et al., 2020 [↗](#)). In the late phase of the

developmental cycle, RBs asynchronously condense into EBs, and this process is termed secondary differentiation. Despite these well-defined differences between chlamydial morphological forms, how *Chlamydia* mechanistically differentiates between functional forms remains unclear.

Intriguingly, a recent study evaluated the redox potential of *Chlamydia* and demonstrated that RBs are reduced, whereas EBs are oxidized (Wang et al., 2014 [↗](#)). This is consistent with earlier studies that revealed differences in the crosslinking of outer membrane proteins and type III secretion-related proteins in chlamydial developmental forms (Betts-Hampikian & Fields, 2011 [↗](#); Caldwell et al., 1981 [↗](#); Everett & Hatch, 1995 [↗](#); Wang et al., 2014 [↗](#)). Taken together, these observations indicate that, during the developmental cycle, the redox potential of the bacteria is changing. However, whether redox changes in the bacteria directly affect developmental cycle progression is not characterized. Based on the different redox status of the chlamydial developmental forms, we hypothesized that increasing the oxidation of the RB drives secondary differentiation to the EB. We used chlamydial transformants designed to overexpress or reduce AhpC levels to explore the effects of altered redox potential in chlamydial growth and development to test this hypothesis. This study establishes the role of AhpC as an antioxidant in *Chlamydia*, as demonstrated by its ability to counteract different peroxide stresses when overexpressed. Overexpression of AhpC had no negative effect on bacterial replication but delayed the differentiation of RBs to EBs. In contrast, under conditions of *ahpC* knockdown, the organism was highly sensitive to oxidizing conditions. Interestingly, this change in redox potential caused earlier expression of EB-associated (late) genes and production of EBs, leading to a shift in developmental cycle progression. This earlier activation of gene expression related to secondary differentiation in *ahpC* knockdown was also observed when developmental cycle progression was blocked by penicillin treatment. Taken together these data provide mechanistic insight into chlamydial secondary differentiation and are the first to demonstrate redox-regulated differentiation in *Chlamydia*.

## Results

### The redox threshold hypothesis and chlamydial secondary differentiation

The chlamydial EB and RB developmental forms differ in size, infectivity, and division capacity. In addition to these characteristics, both forms also differ in their redox status: EBs are oxidized and RBs are reduced (Fig. 1A [↗](#)). Based on this information, we hypothesized that changing redox potential is a critical factor in the process of differentiation from one form to the other. We named this the “redox threshold hypothesis”. In this scenario, as soon as a given RB has crossed an oxidative threshold, the activity of critical proteins is modified to trigger differentiation to the EB (Fig. 1B [↗](#)). AhpC is an antioxidant enzyme, and several reports have indicated that ablation of *ahpC* creates highly oxidized conditions in bacteria (Feng et al., 2020 [↗](#); Zhang et al., 2019 [↗](#)). Therefore, we hypothesize that AhpC, which maintains redox homeostasis in other bacteria, is a critical factor in mediating developmental cycle progression and that altering its activity will impact developmental cycle progression consistent with the redox threshold hypothesis (Fig. 1C [↗](#)).

### Overexpression of *ahpC* has minimal impact on chlamydial growth

To study the effect of AhpC on chlamydial developmental cycle progression, we first generated an *ahpC* overexpression (OE) strain using a plasmid encoding an anhydrotetracycline (aTc)-inducible *ahpC* (untagged) and transformed it into a *C. trachomatis* L2 strain lacking its endogenous plasmid (-pL2). The same plasmid vector backbone (i.e., encoding mCherry in place of *ahpC*) was used as an empty vector control (EV). HeLa cells were infected with these transformants, and, at 10 hpi, expression of the construct was induced or not. Lacking an antibody against AhpC, overexpression

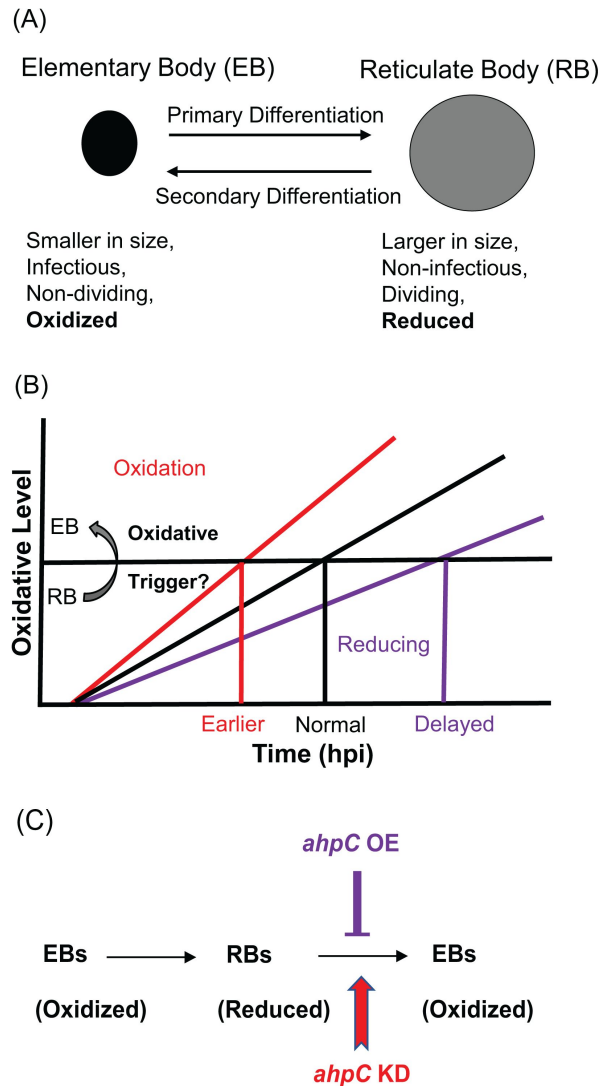


**Fig. 1**

Alterations in redox status of key proteins regulate and drive chlamydial differentiation. (A) Key characteristics of chlamydial developmental forms. (B) Hypothetical model for triggering secondary differentiation through oxidative stress (black angled line). Increasing oxidation of critical protein(s) may lead to earlier differentiation whereas maintaining a reducing environment may delay differentiation. (C) Schematic representation of experimental model for triggering secondary differentiation through altered activity of AhpC. *ahpC* knockdown may lead to earlier differentiation while overexpression of *ahpC* may delay differentiation.

of *ahpC* was validated by reverse transcription-quantitative PCR (RT-qPCR). Here, an approximate 1-log increase in transcripts of *ahpC* was detected at 14 and 24 hpi in the induced strain in comparison to the uninduced strain (Fig. 2A [↗](#)).

Immunofluorescence analysis (IFA) was performed at 24 hpi to examine the organisms' morphology and overall inclusion growth. For IFA, individual bacteria were labeled with an anti-*ahpC* increased the overall inclusion area (Fig. 2B [↗](#) and 2C [↗](#)). We next quantified the total number data support the hypothesis that overexpressing *ahpC* delays production of infectious EBs.

## Overexpression of *ahpC* confers resistance to peroxides in *Chlamydia*

AhpC is an important peroxiredoxin involved in oxidative damage defense. Before determining whether increased *ahpC* expression impacts chlamydial sensitivity to oxidizing agents, we first sought to determine the response of *C. trachomatis* to inorganic or organic hydroperoxides such as hydrogen peroxide ( $H_2O_2$ ), cumene hydroperoxide (CHP), and tert-butyl hydroperoxide (TBHP) as well as peroxyxynitrite (PN). To do this, we evaluated the sensitivity of HeLa cells, infected or not with the empty vector (EV) control strain, to different concentrations of oxidizing agents using a viability assay. Both uninfected and EV-infected HeLa cells tolerated up to 1 mM oxidizing agents for 30 min (Fig. S1). Next, different concentrations (lower than 1 mM) of these oxidants were tested on wild-type (WT) *C. trachomatis* L2/434/Bu (Ctr L2). HeLa cells were infected with Ctr L2 and, at 16 hpi, were exposed to different concentrations of exogenous oxidizing agents for 30 min only, before washing out the oxidizing agents and replacing the media. Samples for IFU and IFA assays were then collected at 24 hpi to assess effects of the oxidizing agents on growth of Ctr L2. 62.5  $\mu$ M concentration of all three inorganic and organic peroxides had no appreciable effect on IFUs, and inclusion size and morphology also remained unaffected at this sublethal concentration. The concentrations of inorganic and organic peroxides that resulted in a decrease in IFUs to ~50% of the untreated culture were 500  $\mu$ M ( $H_2O_2$ ) and 250  $\mu$ M (CHP and TBHP), respectively, with a concurrent decrease in inclusion size. 1 mM  $H_2O_2$ , CHP, and TBHP caused >90% reduction in IFUs and small inclusions. PN at 1 mM concentration was less effective than other oxidizing agents and showed only a ~30% decline in IFUs compared to the untreated culture (Fig. S2).

To further examine the antioxidant functions of AhpC, we next exploited our *ahpC* overexpression strain to explore its capability to protect chlamydiae from oxidizing agents. Both *ahpC* OE and EV strains were used to infect HeLa cells and, at 10 hpi, expression of the constructs was induced or not with 1 nM aTc. At 16 hpi, infected cells were exposed to various concentrations of exogenous oxidizing agents for 30 min. At 24 hpi, IFU and IFA samples were collected to measure chlamydial growth and assess chlamydial morphology, respectively. As shown in Figure 3A [↗](#), 3B, and S3, the *ahpC* overexpression strain showed increased resistance to all oxidants tested as the mean IFUs and the size of inclusions were greater than that of the uninduced but treated control. There was no change in bacterial growth and morphology in the case of 62.5  $\mu$ M concentrations of oxidizing agents, which was anticipated since we determined this was a sublethal concentration. The resistant phenotype was more evident at the higher concentrations of  $H_2O_2$ , CHP, and TBHP. Overexpression of *ahpC* also contributed to higher resistance against PN. Conversely, the empty vector control strain behaved as expected (i.e., like WT) in the presence of oxidizing agents, with similar results observed in the presence or absence of aTc (Fig. 3C [↗](#), 3D [↗](#), and S3). Collectively, these data demonstrate that the chlamydial AhpC possesses antioxidant activity, as expected, and that increased *ahpC* expression is protective for *Chlamydia* in the presence of increased oxidative stress.

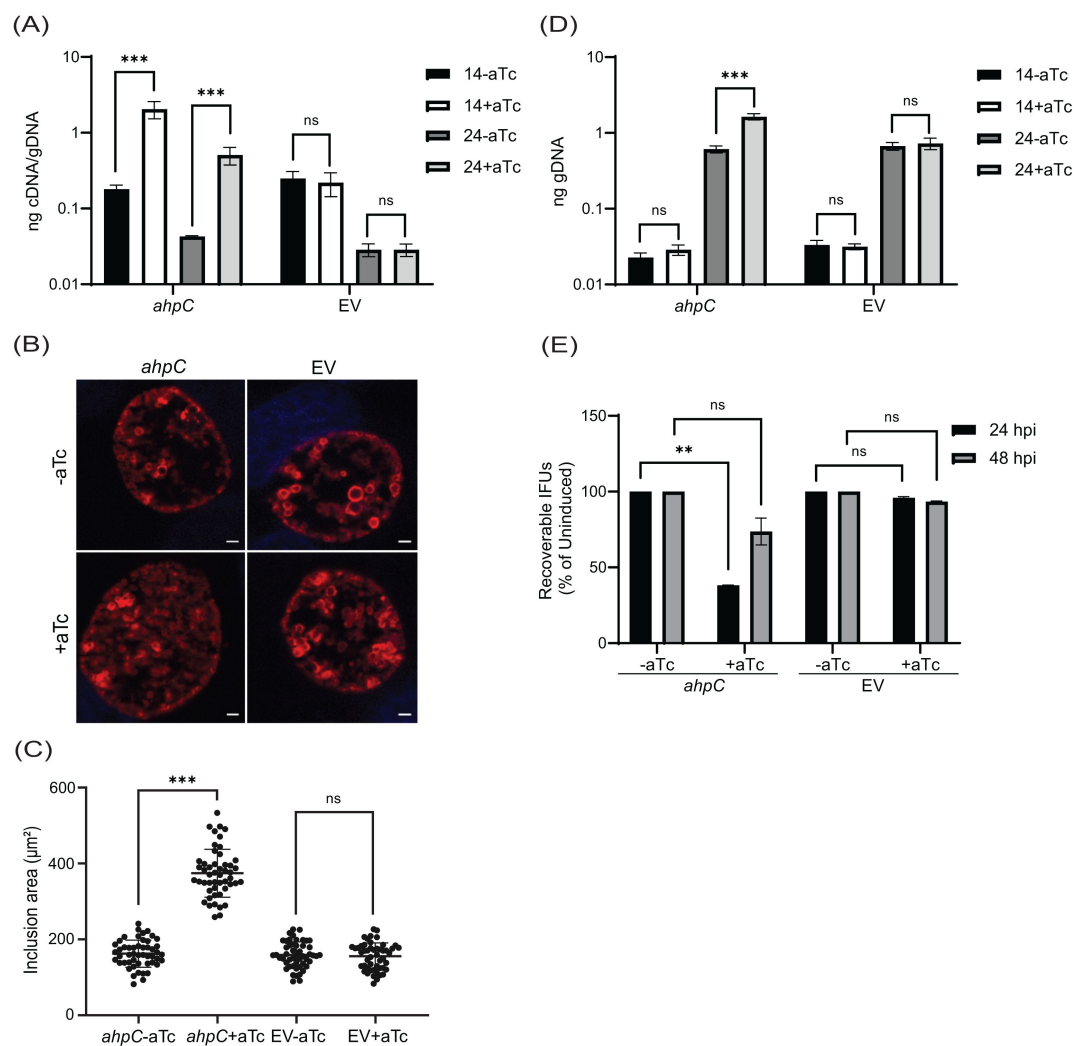


**Fig. 2**

Overexpression of *ahpC* affects chlamydial growth and differentiation. (A) Transcriptional analysis of *ahpC* in *ahpC* overexpression (*ahpC*) and empty vector (EV) control using RT-qPCR following induction at 10 hpi with 1 nM aTc. RNA and genomic DNA (gDNA) were harvested at 14 and 24 hpi and processed as mentioned in materials and methods. Data are presented as a ratio of cDNA to gDNA plotted on a log scale. \*\*\* $p < 0.0001$  vs uninduced sample by using two-way ANOVA. Data represent three biological replicates. (B) Immunofluorescence assay (IFA) of *ahpC* and EV at 24 hpi. Construct expression was induced or not at 10 hpi with 1 nM aTc, and samples were fixed with methanol at 24 hpi then stained for major outer membrane protein (MOMP - red) and DAPI (blue) to label DNA. Scale bars = 2  $\mu$ m. Images were captured using a Zeiss Axio Imager Z.2 with Apotome2 at 100x magnification. Representative images of three biological replicates are shown. (C) Impact of *ahpC* overexpression on inclusion area. Inclusion area of *ahpC* overexpression and EV strains was measured using ImageJ. Experimental conditions were the same as mentioned in section (B). The area of 50 inclusions was measured per condition for each sample. \*\*\* $p < 0.001$  vs uninduced sample by using ordinary one-way ANOVA. Data were collected from three biological replicates. (D) IFU assay of *ahpC* overexpression and empty vector control. Expression of the construct was induced or not at 10 hpi, and samples were harvested at 24 or 48 hpi for reinfection and enumeration. IFUs were calculated as the percentage of uninduced samples. \*\* $p < 0.001$  vs uninduced sample by using multiple paired t test. Data represent three biological replicates. (E) Quantification of genomic DNA (gDNA) determined by qPCR in *ahpC* overexpression and empty vector control. Construct expression was induced or not at 10 hpi with 1 nM aTc, gDNA was harvested at 14 and 24 hpi, and ng gDNA were plotted on a log scale. \*\*\* $p < 0.0001$  vs uninduced sample by using two-way ANOVA. Data represent three biological replicates.

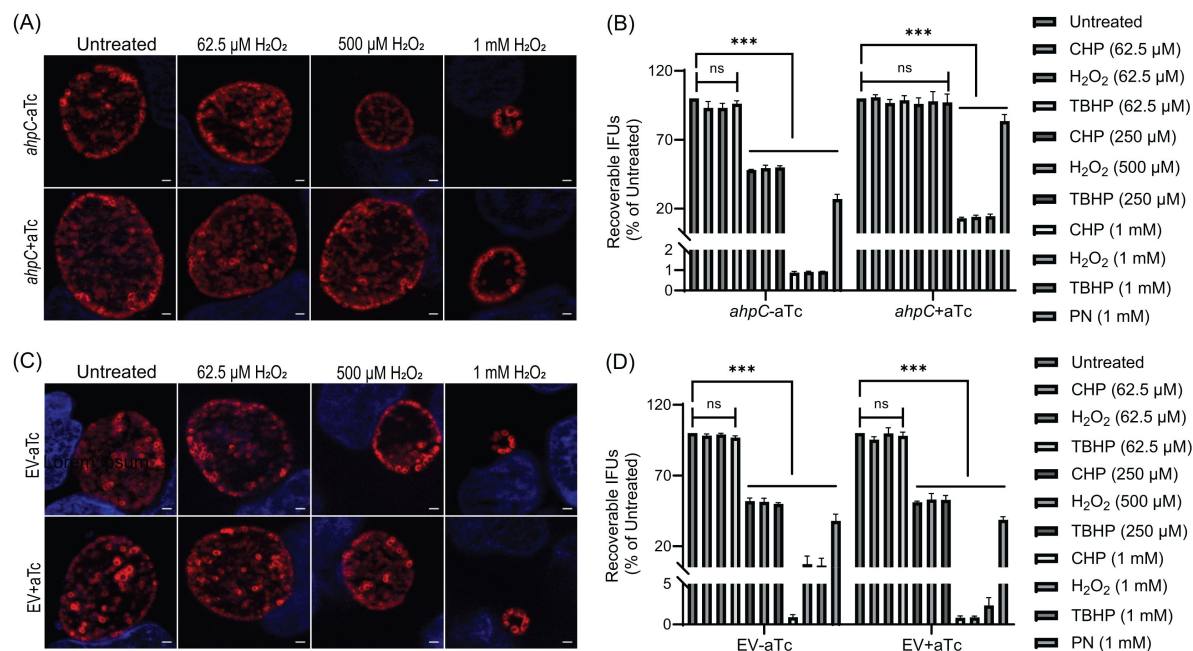


**Fig. 3**

Higher expression of *ahpC* provides resistance to peroxides in *Chlamydia*. IFA of *ahpC* (A) or EV (C) exposed to oxidizing agents. Construct expression was induced or not at 10 hpi with 1 nM aTc, and samples were treated with three different concentrations of hydrogen peroxide ( $\text{H}_2\text{O}_2$ ) at 16 hpi for 30 min then fixed with methanol at 24 hpi and stained and imaged as described in the legend of **Fig. 2B**. Representative images from three biological replicates are shown. IFU analysis of *ahpC* (B) or EV (D) following treatment with oxidizing agents, CHP-Cumene hydroperoxide,  $\text{H}_2\text{O}_2$ -Hydrogen peroxide, TBHP-Tert-butyl hydroperoxide, and PN-Peroxynitrite. Samples were processed as described for (A) and (C), and IFUs harvested at 24 hpi. IFUs of treated samples were compared with respective untreated controls. \*\*\* $p < 0.0001$  vs untreated sample by using two-way ANOVA. Data represent three biological replicates.

## Knockdown of *ahpC* negatively impacts chlamydial growth

To further define the function(s) of AhpC in the chlamydial developmental cycle, we used a novel dCas12-based CRISPR interference (CRISPRi) strategy adapted for *Chlamydia* by our lab (Ouellette, 2018; Ouellette et al., 2021). We generated an *ahpC* knockdown strain harboring the pBOMBL12CRia with a crRNA targeting the *ahpC* 5' intergenic region (plasmid designated as pL12CRia(*ahpC*)). We used a strain carrying a pL12CRia plasmid with a crRNA with no homology to any chlamydial sequence (i.e., non-targeting [NT]) to serve as a negative control. To confirm the knockdown of *ahpC*, RT-qPCR was employed. Here, we infected HeLa cells with the *ahpC* knockdown (*ahpC* KD) or NT strains and induced dCas12 expression or not at 10 hpi using 1 nM aTc. Nucleic acid samples were harvested at 14 hpi and 24 hpi. RT-qPCR analysis of the *ahpC* KD revealed approximately 90% reduction of *ahpC* transcripts compared to the uninduced control, thus confirming the knockdown of *ahpC* (Fig. 4A). In the case of the NT control, there was no effect on *ahpC* transcripts. IFA of these strains revealed noticeably smaller inclusions after blocking expression of *ahpC* as compared to the uninduced sample or the NT conditions (Fig. 4B). We next measured total bacterial counts using genomic DNA. Surprisingly, even though inclusions were smaller during *ahpC* knockdown, we observed slightly higher gDNA levels at 14 hpi compared to the uninduced control, followed by only a small increase from 14 to 24 hpi (Fig. 4C). In contrast, the uninduced strain showed a logarithmic increase in gDNA levels during this timeframe. These effects were not detected for the NT strain (Fig. 4C). To further explore the effect of reduced *ahpC* transcripts in *Chlamydia*, IFU assays were performed. IFU analysis exhibited severely reduced progeny (>90%) in *ahpC* knockdown compared to its respective uninduced control at both time points assessed (24 and 48 hpi) (Fig. 4D). In contrast, the NT strain showed less than a 50% reduction after inducing dCas12 expression at these timepoints consistent with prior observations that dCas12 expression slightly delays developmental cycle progression (Hatch & Ouellette, 2023; Reuter et al., 2023). Taken together, these analyses indicate that reducing *ahpC* levels and/or activity severely disrupted chlamydial growth and development.

To investigate whether *ahpC* knockdown resulted in increased ROS levels in the bacteria (Zhang et al., 2019), the intracellular ROS levels were measured in infected cells in *ahpC* knockdown conditions and compared to the uninduced control condition and uninfected cells. We used the cell-permeable, fluorogenic dye CellROX Deep Red to measure ROS levels. This dye remains non-fluorescent in a reduced state and exhibits bright fluorescence once oxidized by ROS. ROS generation was measured in uninfected and *ahpC* KD-infected HeLa cells at 24 and 48 hpi. As shown in Figure 4E, *ahpC* knockdown resulted in significantly higher ROS than the uninfected or infected but uninduced samples at both 24 hpi and 48 hpi time points. These results together indicate that AhpC plays an important role in counteracting oxidative stress by reducing ROS in *C. trachomatis*.

## Knockdown of *ahpC* sensitizes *Chlamydia* to oxidizing agents

As overexpression of *ahpC* resulted in increased resistance to oxidizing agents, we next explored whether knockdown of *ahpC* resulted in increased sensitivity to such agents. As described above, *ahpC* KD and NT strains were used to infect HeLa cells and, at 10 hpi, expression of dCas12 was induced or not with 1 nM aTc. Considering that the *ahpC* KD already demonstrated reduced IFUs and inclusion sizes at 24 hpi, only sublethal concentrations (62.5  $\mu$ M) of exogenous oxidizing agents were applied. At 24 hpi, IFA and IFU analyses were performed to quantify the effect of the oxidants on chlamydial growth in the absence of *ahpC* activity. Under conditions of *ahpC* knockdown, even sublethal concentrations (62.5  $\mu$ M) of H<sub>2</sub>O<sub>2</sub>, CHP, or TBHP further reduced the inclusion size, and the IFU data revealed a decrease from >90% to <30% in comparison to the untreated control (Fig. 5A, 5B, and S4). Reduced expression of *ahpC* also affected the survival of *Chlamydia* against peroxynitrite. Notably, there was no significant change in the NT control

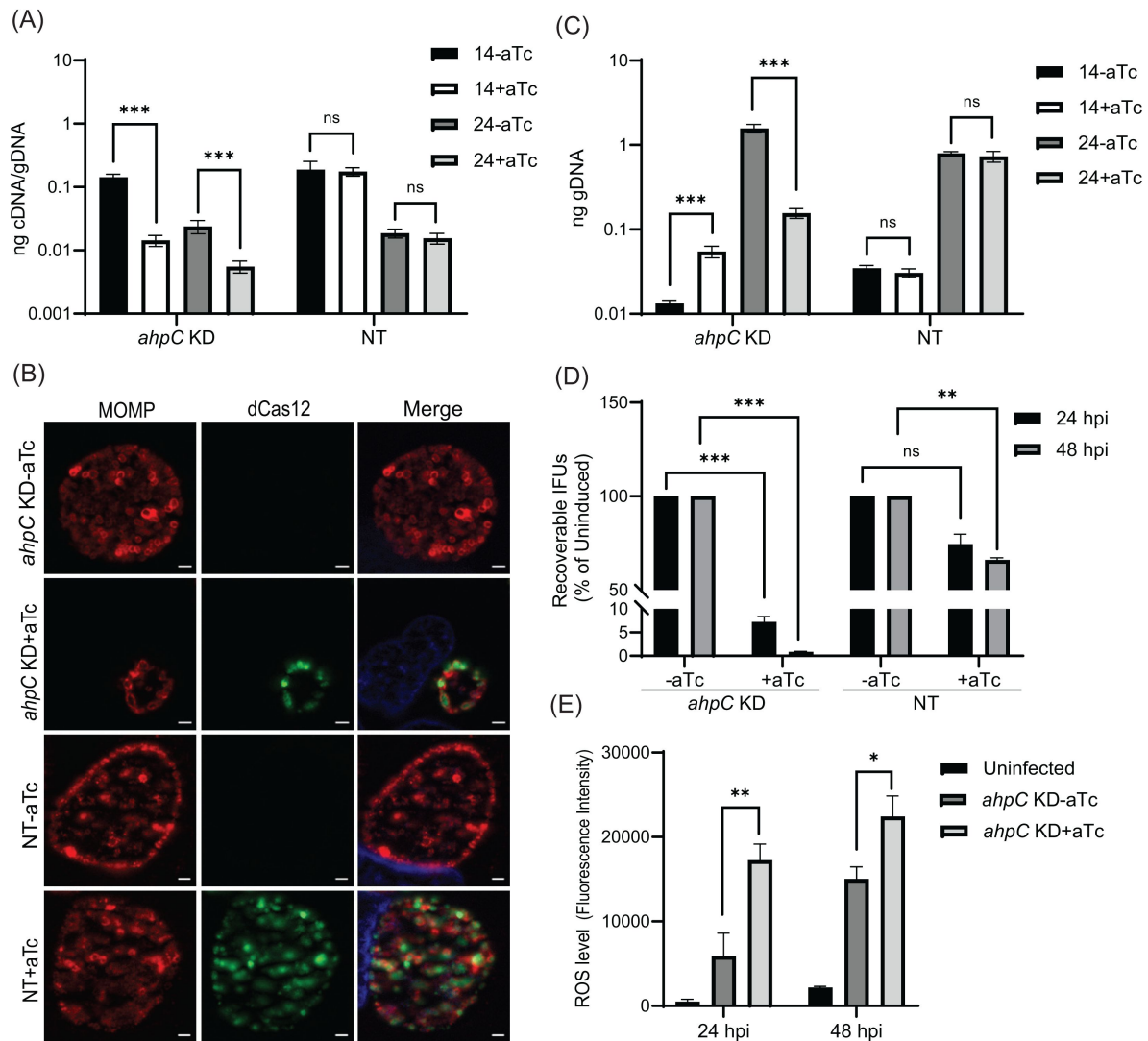


**Fig. 4**

Reduced levels of AhpC negatively impact chlamydial growth. (A) Transcriptional analysis of *ahpC* in knockdown (*ahpC* KD) and non-target (NT) control using RT-qPCR following induction at 10 hpi with 1 nM aTc. RNA and gDNA were harvested at 14 and 24 hpi. Quantified cDNA was normalized to gDNA, and values were plotted on a log scale. \*\*\* $p < 0.0001$  vs uninduced sample by using two-way ANOVA. Data represent three biological replicates. (B) IFA was performed to assess inclusion size and morphology using the same induction conditions as in section (A). At 24 hpi, cells were fixed with methanol and stained using primary antibodies to major outer membrane protein (MOMP), Cpf1 (dCas12), and DAPI. All images were acquired on Zeiss Axio Imager Z.2 with Apotome2 at 100x magnification. Bars, 2 μm. Representative images of three biological replicates are shown. (C) Quantification of genomic DNA (gDNA) determined by qPCR in *ahpC* KD and NT strains. dCas12 expression was induced or not at 10 hpi, and gDNA was harvested at 14 and 24 hpi and plotted on a log scale. \*\*\* $p < 0.0001$  vs uninduced sample by using two-way ANOVA. Data represent three biological replicates. (D) IFU titers following induction at 10 hpi with 1 nM aTc. IFUs were counted from 24 and 48 hpi samples and calculated as percentage of uninduced samples. \*\*\* $p < 0.0001$ , \*\* $p < 0.001$  vs uninduced sample by using multiple paired t test. Data represent three biological replicates. (E) Intracellular ROS levels were measured to investigate the function of AhpC in reducing ROS. HeLa cells were infected or not with *ahpC* knockdown, and knockdown was induced or not at 10 hpi with 1 nM aTc. At 24 hpi, samples were washed with DPBS and incubated with CellROX Deep red dye for 30 min in dark. ROS levels were measured at wavelengths of 640nm (excitation) and 665nm (emission). \*\* $p < 0.001$ , \* $p < 0.01$  vs uninduced sample by using two-way ANOVA. Data represent three biological replicates.

strain in the uninduced and induced samples in response to oxidizing agents as assessed by IFU and IFA (Fig. 5C, 5D, and S4). These data further support that the chlamydial AhpC is a critical antioxidant enzyme in these bacteria.

## Complementation restores the growth and resistance to low levels of peroxide stress of the *ahpC* knockdown strain

To validate that the impaired growth, altered inclusion morphology, and enhanced sensitivity to peroxides were due to the decreased level/activity of AhpC, we generated a complemented strain of *ahpC* knockdown. For the construction of the *ahpC* complementing plasmid, the *ahpC* gene was cloned and transcriptionally fused 3' to the dCas12 in the pL12CRia(*ahpC*) knockdown plasmid. Here, the complementing *ahpC* allele is also under the control of the aTc-induced *Ptet* promoter and is co-expressed with the aTc-inducible dCas12. Consequently, the *ahpC* knockdown effect is ablated, and the observed phenotypes should be restored. After inducing dCas12-*ahpC* expression with aTc, the resultant strain was verified by RT-qPCR. Increased transcripts for *ahpC* were quantified under these conditions, indicating successful complementation of the knockdown effect (Fig. 6A). Of note, the *ahpC* transcript levels remained elevated in comparison to the uninduced control at the 24hpi time point. After confirming this strain, we measured genomic DNA to quantify total bacteria and performed IFA and IFU assays to examine if complementation restored the phenotypes observed during *ahpC* knockdown. These assays revealed normal inclusion morphology, gDNA levels, and EB progeny production in the complemented strain, indicating successful complementation of the knockdown phenotype (Fig. 6B, C, and D). Of note, a C-terminal 6xHis tagged AhpC was not capable of complementing the knockdown phenotype (data not shown), indicating a requirement for a free C-terminus in the function of AhpC in *Chlamydia*. Previous studies in other bacteria have revealed that the C-terminal residues in AhpC play a crucial role in the structural stability and enzymatic activity of AhpC (Dip et al., 2014; Feng et al., 2020; Wan et al., 2021).

We next assessed whether complementation of the knockdown phenotype could also restore the resistance to low levels of peroxide stress. As in previous experiments, a sublethal concentration of oxidizing agents was added for 30' at 16 hpi after having induced dCas12-*ahpC* expression at 10 hpi. Consistent with the growth parameters (Fig. 6B-D), the complemented strain showed wild-type responses in these conditions (Fig. 6E, 6F, and S4). These data indicate that the enhanced susceptibility of the *ahpC* knockdown strain to oxidizing agents was due to the reduced levels of *ahpC* and not an indirect effect of knockdown.

We predicted that the growth defects resulting from higher production of ROS during *ahpC* knockdown could be rescued by treating the *ahpC* KD with ROS scavengers. To test this prediction, we utilized two characterized ROS scavengers, DMTU (*N,N*-dimethylthiourea) and  $\alpha$ -tocopherol, which scavenge  $H_2O_2$  and peroxy radical, respectively (Hollander-Czytko et al., 2005; Kiffin et al., 2006; Walch et al., 2015). First, the effect of ROS scavengers on uninfected and infected HeLa cells was investigated using a viability assay. This assay revealed that 10 mM DMTU and 100  $\mu$ M  $\alpha$ -tocopherol had no adverse effects on uninfected or EV-infected HeLa cells (data not shown). These same concentrations were tested on WT *Ctr* L2 infected HeLa cells in untreated and 500  $\mu$ M  $H_2O_2$  treated conditions to test the potency of these scavengers to rescue growth defects associated with this concentration of oxidizing agent. Scavengers were added at 9.5 hpi and washed away at 16 hpi - the time of addition of  $H_2O_2$  in the respective samples. At 16.5 hpi, after 3 wash steps, scavengers were added again with fresh media, and, at 24 hpi, bacterial growth and morphology were assessed using IFU and IFA assays. Neither scavenger had a significant impact on chlamydial morphology or infectious progeny. In the case of peroxide (500  $\mu$ M  $H_2O_2$ ) treated samples, scavengers restored IFUs from ~50% to ~100%, and inclusion size was also recovered (Fig. S5A and B).

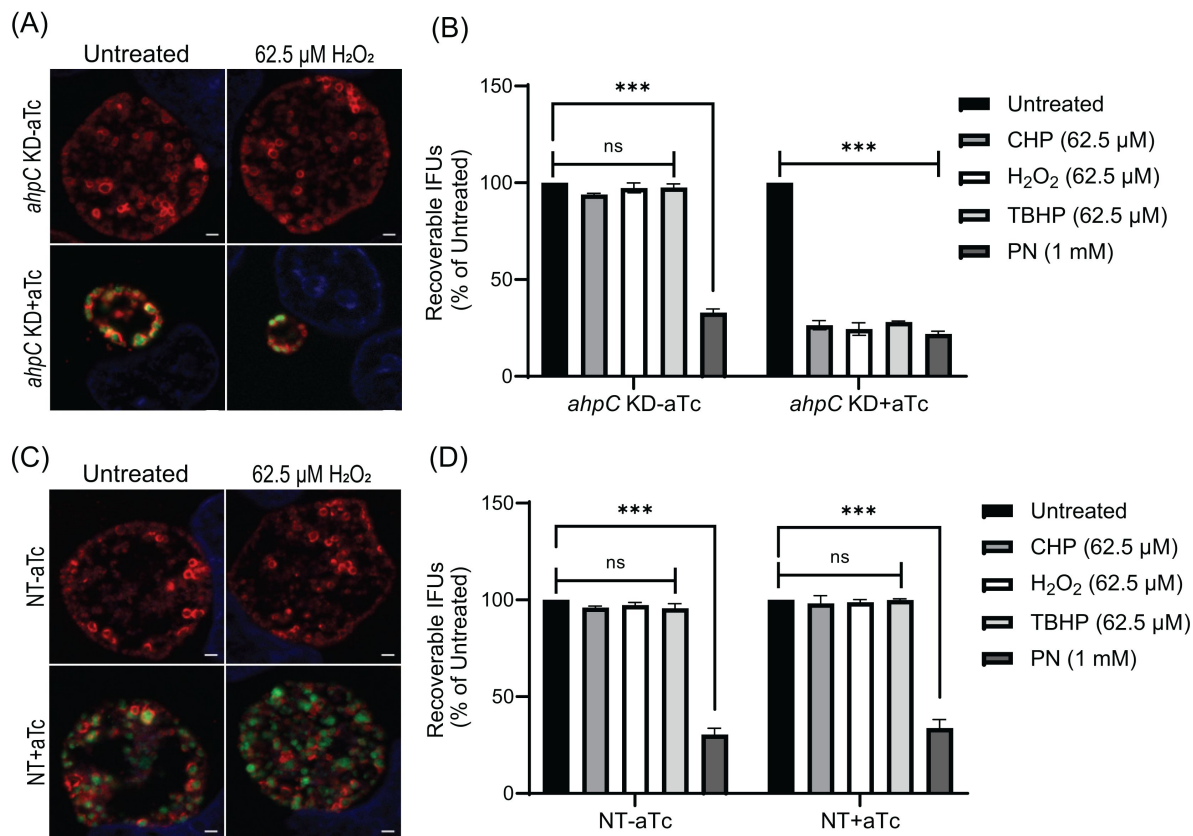


**Fig. 5**

*Chlamydia* is hypersensitive to oxidizing agents in *ahpC* knockdown condition. IFA of *ahpC* KD (A) or NT (C) treated with 62.5  $\mu$ M  $H_2O_2$ . dCas12 expression was induced or not at 10 hpi with 1 nM aTc, treated or not with  $H_2O_2$  at 16 hpi for 30 min, and allowed to grow until 24 hpi. Coverslips were fixed with methanol at 24 hpi and stained major outer membrane protein (MOMP), Cpf1 (dCas12), and DAPI. Scale bars = 2  $\mu$ m. Images were captured using a Zeiss Axio Imager Z.2 with Apotome2 at 100x magnification. Representative images from three biological replicates are shown. IFU analysis of *ahpC* KD (B) or NT (D) following treatment with oxidizing agents, CHP-Cumene hydroperoxide,  $H_2O_2$ -Hydrogen peroxide, TBHP-Tert-butyl hydroperoxide, or PN-Peroxynitrite. dCas12 expression was induced or not, and samples were treated or not as mentioned in the legend of **Fig. 3B**. IFUs of treated samples were calculated as percentage of respective untreated samples. \*\*\*p < 0.0001 vs untreated sample by using two-way ANOVA. Data represent three biological replicates.

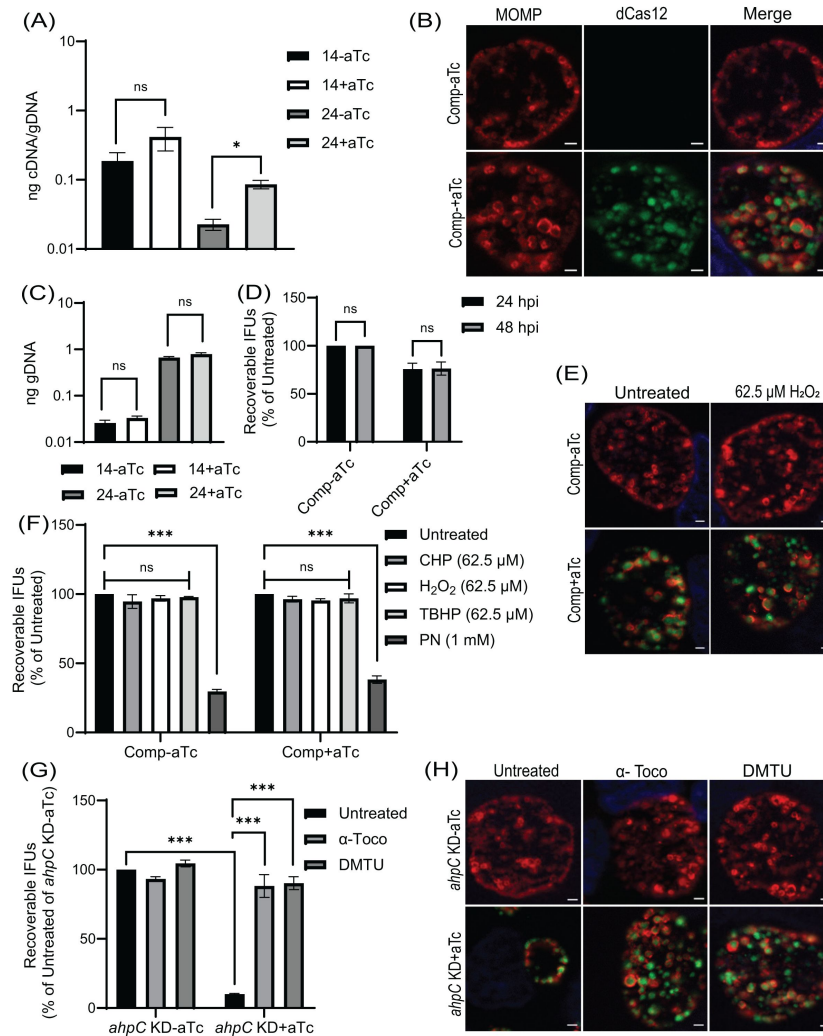


**Fig. 6**

Complementation of the phenotypes observed in the *ahpC* knockdown. (A) Confirmation of complementation (comp) of *ahpC* knockdown by RT-qPCR. Samples were processed and quantified as mentioned previously in the legend of **Fig. 4A**. Values were plotted on a log scale. \* $p < 0.01$  vs uninduced sample using ordinary one-way ANOVA. Data represent three biological replicates. (B) IFA of comp strain was performed at 24 hpi, and staining and imaging were performed as mentioned in the legend of **Fig. 4B**. Scale bars, 2  $\mu\text{m}$ . Representative images from three biological replicates are shown. (C) Genomic DNA quantitation was performed by qPCR. Construct expression was induced or not at 10 hpi, and gDNA was harvested at 14 and 24 hpi and plotted on a log scale. Statistical analysis was calculated using ordinary one-way ANOVA. Data represent three biological replicates. (D) IFU analysis of comp strain. Statistical analysis was calculated using multiple paired t test. Data represent three biological replicates. (E) IFA of comp strain following treatment with 62.5  $\mu\text{M}$   $\text{H}_2\text{O}_2$ . Samples were treated, stained, and images acquired as mentioned in the legend of **Fig. 5A**. Scale bars = 2  $\mu\text{m}$ . Representative images from three biological replicates are shown. (F) IFU analysis of comp strain following treatment with oxidizing agents. Experiments were performed as mentioned in the legend of **Fig. 5B**. IFUs were calculated as percentage of respective untreated samples. \*\*\* $p < 0.0001$  vs untreated sample by using two-way ANOVA. Data represent three biological replicates. (G) *ahpC* knockdown growth defect rescued by ROS scavengers. IFU analysis of *ahpC* knockdown treated with or without scavengers,  $\alpha$ -Tocopherol (100  $\mu\text{M}$ ) and DMTU (10 mM), as mentioned in materials and methods. IFUs were calculated as a percentage of the untreated, uninduced sample. \*\*\* $p < 0.0001$  vs untreated, uninduced or induced sample by using two-way ANOVA. Data represent three biological replicates. (H) IFA of *ahpC* knockdown treated with or without scavengers. Experimental conditions were similar as in section (G). Staining and imaging were performed as mentioned in **Fig. 5A**. Representative images from three biological replicates are shown.

Next, the effect of the ROS scavengers under *ahpC* knockdown conditions was assessed. In this experiment, scavengers were added at 9.5 hpi to provide the protective effect of scavengers before reducing the activity of *ahpC*. At 10 hpi, knockdown was induced or not with 1 nM aTc, and, at 14 hpi, scavengers were added again. At 24 hpi, IFU and IFA samples were collected to examine bacterial growth and morphology to assess the effect of ROS scavenging on the *ahpC* knockdown phenotype. As shown in **Fig. 6G** and **6H**, both ROS scavengers had a positive impact on restoring growth of the *ahpC* knockdown strain; inclusions were larger, and IFUs were increased from <10% to >90% in the presence of scavengers in the induced samples. These data provide compelling evidence that the adverse effects of *ahpC* knockdown are due to increased ROS accumulation in this strain.

## Chlamydial developmental cycle progression is altered by *ahpC* knockdown/ overexpression

Whereas the overexpression of AhpC delayed overall developmental progression and was consistent with our hypothesis, the results with the *ahpC* knockdown strain appeared to refute our hypothesis given the apparent decrease in IFUs and smaller inclusion sizes after knockdown. To investigate the effects of changes in redox potential on chlamydial developmental cycle progression, we performed a transcriptional analysis of well-characterized late-cycle genes associated with secondary differentiation (*hctA*, *hctB*, *glgA*, *tsp*, and *omcB*) (Belland et al., 2003; Gehre et al., 2016; Newhall, 1987; Ouellette et al., 2006; Swoboda et al., 2023). In the uninduced samples, transcript levels of all the tested late genes were higher at 24 hpi compared to 14 hpi, indicating their normal expression during the late stage of the developmental cycle. In comparison to the uninduced control, under conditions of *ahpC* knockdown, significantly higher expression of *hctA*, *hctB*, *omcB*, *tsp*, and *glgA* was observed at the mid-developmental cycle timepoint of 14 hpi (**Fig. 7A**). At 24 hpi, expression of these genes was comparable between the uninduced and induced conditions in the *ahpC* knockdown strain. In contrast, the complementation strain showed no increase in the expression of these tested late genes at 14 hpi, and *tsp* and *glgA* transcripts were reduced (**Fig. 7C**). Consistent with our model, the overexpression of *ahpC* resulted in significantly lower expression of *hctA*, *hctB*, *omcB*, *tsp*, and *glgA* at 14 and 24 hpi (**Fig. 7D**), suggesting a delayed transition to EBs.

Given the increase in late gene expression during *ahpC* knockdown at an earlier time point in the developmental cycle than normal, we reasoned that the increase in oxidizing conditions might prematurely trigger secondary differentiation and EB production. However, complicating such an analysis is that fewer RBs are present to convert to EBs, which would result in overall lower IFU yields as we had measured at 24 and 48 hpi (**Fig. 4D**). Nonetheless, to assess EB production more rigorously at earlier time points in the developmental cycle, we performed a growth curve analysis to precisely measure IFUs at two-hour intervals from 16 to 24 hpi. HeLa cells were infected, and knockdown was induced or not at 10 hpi with 1 nM aTc. At the indicated time points, IFU samples were collected and quantified. Consistent with our prediction, this experiment revealed higher IFUs (i.e., EBs) at 16 and 18 hpi during *ahpC* knockdown compared to the uninduced samples (**Fig. 7B**). This difference was statistically significant at 18 hpi. However, further EB production was stalled, with the uninduced strain continuing to produce EBs such that, by 24 hpi, there were significantly higher EB yields under these conditions (as noted in **Fig. 4D**). These data show that the phenotypic consequence of higher expression at 14 hpi of genes functionally related to EBs is the concomitant earlier production of EBs. These data underscore that reduced activity of *ahpC* causes earlier secondary differentiation in *C. trachomatis*.

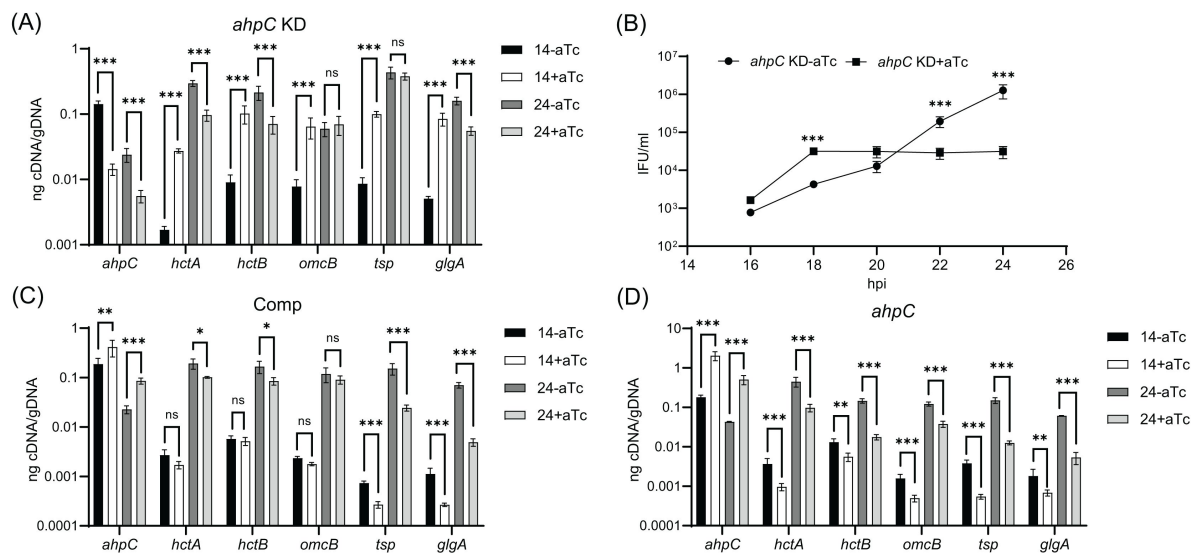


**Fig. 7**

Effects of *ahpC* knockdown/overexpression on chlamydial developmental cycle progression. RT-qPCR analysis of late cycle genes (*hctA*, *hctB*, *omcB*, *tsp*, and *glgA*) in (A) *ahpC* knockdown, (C) complementation, and (D) *ahpC* overexpression strain. Experimental conditions were the same as mentioned in the legend of **Fig. 4A**. Quantified cDNA was normalized to gDNA, and values were plotted on a log scale. \*\*\* $p < 0.0001$ , \*\* $p < 0.001$ , \* $p < 0.01$  vs uninduced sample by using two-way ANOVA. Data represent three biological replicates. (B) One-step growth curve of *ahpC* knockdown. Samples were induced or not with 1 nM aTc at 10 hpi and harvested at 16, 18, 20, 22, and 24 hpi. IFUs recovered are displayed as log<sub>10</sub> values. \*\*\* $p < 0.0001$  vs uninduced sample by using two-way ANOVA. Data represent three biological replicates.

## ***ahpC* knockdown activates transcription of late-cycle genes when bacterial replication is blocked**

We detected earlier expression of EB-related genes during *ahpC* knockdown and were curious if the *ahpC* knockdown condition could activate these genes under conditions when the chlamydial developmental cycle is blocked. Pathogenic *Chlamydia* species undergo a polarized cell division process, in which peptidoglycan is transiently synthesized only at the division septum (Abdelrahman et al., 2016 [DOI](#); Cox et al., 2020 [DOI](#); Ouellette et al., 2020 [DOI](#)). As a result, during penicillin treatment, division of RBs is blocked (Moulder, 1993 [DOI](#); Moulder et al., 1956 [DOI](#); Ouellette et al., 2020 [DOI](#)). However, the bacteria continue to grow in size resulting in aberrantly enlarged RBs (Barbour et al., 1982 [DOI](#); Matsumoto & Manire, 1970 [DOI](#); Ouellette et al., 2012 [DOI](#)), in which EB-related genes are not transcribed and production of EBs is inhibited (Ouellette et al., 2006 [DOI](#); Panzetta et al., 2018 [DOI](#)).

To examine this, we generated an *ahpC* KD strain with spectinomycin resistance (*ahpC* KD-spec) and validated its phenotype as being the same as the penicillin-resistant *ahpC* KD strain. This new strain, *ahpC* KD-spec, was used to infect HeLa cells, and knockdown was induced or not at 10 hpi with 1 nM aTc. At the same time, samples were treated or not with 1 unit per mL of penicillin (Pen). RNA samples were harvested at 16 and 24 hpi and processed for RT-qPCR (Fig. S6B-D). IFA controls from these different conditions demonstrated the expected phenotypes (Fig. S6A). For example, Pen treatment caused aberrantly enlarged RBs, irrespective of *ahpC* KD, whereas *ahpC* KD itself caused smaller inclusions. Similarly, *ahpC* KD resulted in reduced *ahpC* transcripts in the induced conditions irrespective of the presence of Pen (Fig. S6B). We next quantified transcript levels for the late genes *hctA* and *hctB* in these different conditions (Fig. S6C and D). As expected, in the uninduced and untreated condition, both transcripts had higher expression at 24 hpi, indicating their regular developmental expression during the late stage of the developmental cycle. Consistent with prior observations (Ouellette et al., 2006 [DOI](#)), transcript levels of these genes in uninduced+Pen conditions was low. As we previously noted (Fig. 7A [DOI](#)), the transcripts of *hctA* and *hctB* are higher in the induced than uninduced samples at 16 hpi in the absence of Pen. Interestingly, in the induced+ Pen condition, these genes had higher expression at 24 hpi than the uninduced+Pen control. At 16 hpi, their expression was either higher or similar between both samples (i.e., induced+Pen and uninduced+Pen). Collectively, these data support our observation that *ahpC* knockdown activates the transcription of late-cycle genes – even under conditions where developmental cycle progression is blocked.

## **Discussion**

Secondary differentiation (differentiation from RBs to EBs) is an essential step for chlamydial growth and survival, but there is a dearth of information regarding the mechanisms of its regulation. EBs and RBs have significantly different proteomic repertoires, and our group has identified critical functions for the cytoplasmic ClpXP and ClpCP and periplasmic Tsp proteases during secondary differentiation (Pan, Jensen et al., 2023; Swoboda et al., 2023 [DOI](#); Wood et al., 2022 [DOI](#)). The *tsp* gene, in addition to another late-cycle gene, *hctB*, is transcriptionally regulated by sigma factor 28 ( $\sigma^{28}$ ) (Hatch & Ouellette, 2023 [DOI](#)). Another sigma factor,  $\sigma^{54}$  has been linked to regulation of outer membrane components, type III secretion system components, and other genes typically expressed late in development (Hatch & Ouellette, 2023 [DOI](#); Soules, LaBrie, et al., 2020). In addition to the two minor sigma factors,  $\sigma^{28}$  and  $\sigma^{54}$ , *Chlamydia* encodes one major sigma factor,  $\sigma^{66}$ , which is transcriptionally regulated by the relative levels of RsbV1 (antagonist) and RsbW (anti-sigma factor) (Thompson et al., 2015 [DOI](#)). This Rsb system senses ATP availability and has been proposed to regulate  $\sigma^{66}$  (Thompson et al., 2015 [DOI](#)). A related study from Soules et al. (Soules, Dmitriev, et al., 2020) showed that TCA intermediates act as ligands for RsbU, thereby linking the

Rsb system to the TCA cycle and ATP synthesis. Collectively, these data show that post-translational mechanisms drive secondary differentiation in *Chlamydia*. However, no definitive “switch” that triggers this step has been identified.

Aside from the clear morphological and functional differences between the EB and RB, they also differ in their redox status: EBs are more oxidized whereas RBs are more reduced (Wang et al., 2014). This same study noted that the overall redox status of the host cell was relatively unchanged throughout the developmental cycle, suggesting that changes in the bacteria were driven by endogenous processes (i.e., metabolism). Though *Chlamydia* is dependent on its host for most of its energy requirements, it has some metabolic activities, such as a partial TCA cycle and oxidative phosphorylation (Gerard et al., 2002; Iliffe-Lee & McClarty, 1999) that can be possible sources of intracellular ROS. We hypothesize that accumulating redox stress from its metabolic activities serves as a signal to trigger secondary differentiation from RBs to EBs. There is a paucity of knowledge on how *C. trachomatis* modulates oxidative stress during disease pathogenesis. However, some studies explored the effects of redox changes on *Chlamydia* growth. Boncompain et al. reported that infection of *C. trachomatis* induced the transient production of ROS by the host cell at a moderate level for the initial few hours of infection only (Boncompain et al., 2010). Another study also found a similar observation about ROS during infection, reporting that *Chlamydia* requires host-derived ROS for its growth (Abdul-Sater et al., 2010). Given that no studies have examined the role of chlamydial proteins related to redox and how these proteins impact the growth of the pathogen, we initiated experiments to investigate the function of a key antioxidant enzyme, AhpC, as a means of testing our hypothesis.

Reactive oxygen species (ROS) generation is an inevitable condition for pathogens growing in aerobic conditions, and resistance against oxidative stress (imbalanced level of ROS) is a key survival mechanism (Fang, 2011). Hence, pathogens have evolved detoxifying proteins, such as peroxiredoxins, to eliminate ROS (Dip et al., 2014; Wang et al., 2004; Yang et al., 2002). AhpC is a 2-cys peroxiredoxin and has been reported to have a crucial role in bacterial physiology, survival, and virulence by scavenging ROS and RNI (Cosgrove et al., 2007; Kimura et al., 2012; Loprasert et al., 2003; Oh & Jeon, 2014). In the process of detoxification of peroxides and peroxynitrite, AhpC is converted into an oxidized dimer, requiring alkyl hydroperoxide reductase AhpF or AhpD to regenerate its activity (Koshkin et al., 2004; Poole & Ellis, 1996; Wong et al., 2017). *C. trachomatis* encodes AhpC (Ct603) but lacks any annotated homologs of AhpF or AhpD. Therefore, it remains an open question how AhpC activity is regulated. Some studies have mentioned *ahpC* as an iron-responsive gene in *Chlamydia* (Brinkworth et al., 2018; Pokorzynski et al., 2019), but there is no detailed investigation to date about the role of this crucial antioxidant in the growth and development of *Chlamydia*.

Using a broad set of methodologies, we created and characterized overexpression and knockdown conditions of *ahpC*. Higher expression of *ahpC* resulted in lower EB production at 24 hpi coupled with a higher number of RBs and larger inclusion size (Fig. 2), suggesting differentiation from RBs to EBs is delayed. The number of EBs is further decreased at 48 hpi, but the difference is not statistically significant. This may be due to the highly oxidized conditions in *Chlamydia* at 48 hpi (Wang et al., 2014) or the inability of *ahpC* overexpression to generate sufficient reducing conditions to neutralize it completely. In our studies, *ahpC* expression was induced at 10hpi, and adequate enzyme levels may not have been sustained later during the developmental cycle. Consistent with studies in other bacteria (Sherman et al., 1999; Zuo et al., 2014), overexpression of *ahpC* created resistance to different oxidants (Fig. 3 and S3), indicating that AhpC is the principal defense mechanism against oxidative stress in *Chlamydia*. During *ahpC* knockdown, the attenuated activity of AhpC severely affected the growth of bacteria (Fig. 4). Notably, the morphology of inclusions during *ahpC* knockdown is strikingly similar to *Chlamydia* treated with a high concentration (1 mM) of oxidizing agents (Fig. 4 and Fig S2), indicating similar scenarios in both conditions. This was further supported by the increased sensitivity of

*ahpC* knockdown to sublethal concentrations of oxidants (Fig. 5 and S4). Again, this observation is consistent with previous data from other bacteria (Cosgrove et al., 2007; Seaver & Imlay, 2001; Storz et al., 1989; Zhang et al., 2019).

An essential aspect of the scavenging activity of AhpC for many bacterial pathogens in which it has been studied is that it works best with endogenous (i.e., low) levels of H<sub>2</sub>O<sub>2</sub>. These bacteria, such as *Staphylococcus aureus* and *Yersinia pseudotuberculosis*, encode catalases, which have high K<sub>m</sub> for hydrogen peroxide and serve a predominant role in scavenging exogenous H<sub>2</sub>O<sub>2</sub> (Cosgrove et al., 2007; Wan et al., 2021). Catalases can detoxify H<sub>2</sub>O<sub>2</sub> at high levels (millimolar levels) and are crucial in responding to external H<sub>2</sub>O<sub>2</sub> stress (Mishra & Imlay, 2012). The *ahpC* mutants in these bacteria became sensitive to organic peroxides but resistant to H<sub>2</sub>O<sub>2</sub> due to higher catalase activity as a compensatory response to the lack of AhpC (Antelmann et al., 1996; Mongkolsuk et al., 2000; Ochsner et al., 2000). Further, simultaneous mutations in both catalase and *ahpC* displayed drastically enhanced sensitivity to all oxidizing agents tested (Cosgrove et al., 2007; Ezraty et al., 2017; Seaver & Imlay, 2001). *C. trachomatis* does not encode a catalase gene (Boncompain et al., 2014; Rusconi & Greub, 2013), and hypersensitivity of *ahpC* knockdown to both inorganic and organic peroxides indicates the absence of catalase and establishes that AhpC is the primary scavenger of ROS in *C. trachomatis*. We did not observe significant effects of PN with AhpC expression. One possible explanation may be our study's concentration (1 mM) of PN. Higher concentrations of PN could not be used due to toxic effects on the host cell. The other possibility may be the presence of some other unknown mechanism(s) to detoxify PN. For example, *Chlamydia* also encodes a superoxide dismutase (SOD) that may prevent the accumulation of the necessary precursors that are needed for PN production. We are currently investigating the function of the chlamydial SOD enzyme.

Previous studies in other bacterial systems indicated that ROS production significantly increased after the deletion of *ahpC* (Zhang et al., 2019). Similarly, in *Chlamydia* during *ahpC* knockdown, the ROS level was dramatically higher. Its ability to dissipate ROS produced by exogenous oxidative stress was severely compromised (Fig. 4E). Further, the addition of ROS scavengers to the culture medium rescued the negative phenotypes associated with *ahpC* knockdown (Fig. 6G and H). This strongly suggests that, in the absence of AhpC, higher amounts of reactive oxygen species accumulate in *Chlamydia* and that the negative impact on growth during *ahpC* knockdown is due to highly oxidized conditions in the organism. Moreover, for the complete restoration of inclusion size, multiple doses of scavengers were required throughout the experiment, further emphasizing that the internal chlamydial environment is oxidized and/or susceptible to oxidation in the absence of AhpC. These findings suggest that AhpC in *Chlamydia* is indispensable, having a functional role even more extensive than previously reported in other bacteria.

Interestingly, in our RT-qPCR study, late-cycle genes such as *hctA*, *hctB*, *glgA*, *omcB*, and *tsp* are expressed at a higher level at an earlier time (14 hpi) in the chlamydial developmental cycle as a result of reduced AhpC activity (Fig. 7). Notably, in the developmental cycle of *C. trachomatis*, only RBs are present at 14 hpi, and secondary differentiation starts after 16 hpi (Abdelrahman & Belland, 2005). Expression of most of the late-cycle genes occurs after this time in the developmental cycle (Belland et al., 2003). Among the tested late-cycle genes, *hctA* and *hctB* encode histone-like proteins responsible for chromosomal condensation during the differentiation of RBs into EBs. The *hctA* gene is among the first to be transcribed in the late-stage (Chiarelli et al., 2020). The other three late genes, *tsp*, *omcB*, and *glgA*, are all well-characterized late genes associated with secondary differentiation. Tsp is a periplasmic protease thought to be crucial in the degradation of RB-specific periplasmic proteins during secondary differentiation in *C. trachomatis* (Swoboda et al., 2023). OmcB is responsible for the rigid cell wall and osmotic stability of the EBs (Mygind et al., 1998; Newhall, 1987). GlgA is a non-essential secretory protein involved in glycogen metabolism and is responsible for glycogen accumulation in the inclusion lumen at late stages of the developmental cycle (Gehre et al., 2016; Sun et al., 2020). One crucial point to consider is the redox status of *Chlamydia*. 14 hpi is when reduced RBs

predominate with virtually no oxidized EBs detectable. However, we established that *ahpC* knockdown shifts the redox status of the bacteria towards oxidation. Hence, the earlier and significantly higher detection of transcripts for these late-cycle genes indicate earlier secondary differentiation in the *ahpC* knockdown. Importantly, *ahpC* complementation during knockdown restored the regular developmental expression of these late-cycle genes, further supporting this phenotype was due to the highly oxidized conditions created by reduced AhpC activity.

The higher expression of genes functionally related to EBs and EB production at an early stage of the chlamydial developmental cycle indicates earlier secondary differentiation as an outcome of diminished activity of *ahpC* in *C. trachomatis*. Consequently, increased late gene transcription should have the phenotypic effect of causing earlier production of EBs. Indeed, we quantified more IFUs (proxy for EBs) in the *ahpC* knockdown at 16 and 18 hpi compared to the uninduced control condition. In contrast, for the AhpC overexpression strain, the expression of these late-cycle genes in the induced conditions compared to the uninduced control at 24 hpi is significantly lower, indicating reduced production of EBs. These data support our hypothesis that the developmental cycle is delayed in the reduced environment. We propose a simple model to explain these scenarios (Fig. 8). During *ahpC* KD, higher amounts of ROS accumulation in the bacterium create highly oxidized conditions. As secondary differentiation is asynchronous and RBs divide through an asymmetric budding mechanism (Ouellette et al., 2020), ROS levels are unevenly distributed between mother and daughter cell. This difference will lead some RBs to breach an oxidative threshold sooner, allowing activation of late genes and secondary differentiation earlier than other RBs. In contrast, *ahpC* overexpression scavenges ROS at a greater level leading to a more reducing environment. This results in a delay in achieving the oxidative threshold, thus allowing RBs to continue to divide before committing to secondary differentiation. Taken together, our data directly link oxidation state and secondary differentiation in *Chlamydia*. Ongoing studies are focused on characterizing redox-sensitive chlamydial proteins to understand which specific factors drive the shift from RBs to EBs (or EBs to RBs) in *C. trachomatis*.

## Materials and methods

### Strains and cell culture

For chlamydial transformation, McCoy mouse fibroblast cells (kind gift of Dr. Harlan Caldwell (NIH/NIAID)) were used. Human cervix adenocarcinoma epithelial HeLa cells (kind gift of Dr. Harlan Caldwell (NIH/NIAID)) were used for RT-qPCR, immunofluorescence assays (IFA), inclusion forming unit assays (IFU), viability assays, oxidative stress, ROS measurements, and ROS scavenger assays. Both cell types were routinely grown and passaged in Dulbecco's modified Eagle's medium (DMEM; Gibco, Waltham, MA) supplemented with 10% fetal bovine serum (FBS; Sigma, St. Louis, MO) and 10 µg/mL gentamicin (Gibco, Waltham, MA) at 37°C and 5% CO<sub>2</sub>. All strains were verified to be Mycoplasma-negative using LookOut mycoplasma PCR detection kit (Sigma). For chlamydial transformations, *Chlamydia trachomatis* serovar L2 EBs lacking the endogenous pL2 plasmid (kind gift of Dr. Ian Clarke, University of Southampton) were used (Wang et al., 2011). Wild-type, density gradient-purified *Chlamydia trachomatis* 434/Bu (ATCC VR902B) EBs were used for sensitivity to oxidizing agents and ROS scavenger assays. Molecular biology reagents, oxidizing agents, scavengers, and CellROX Deep Red dye were purchased from Thermo Fisher unless otherwise noted.

### Plasmid construction

The primers, gBlock gene fragments, plasmids, and bacterial strains used for molecular cloning are listed in Table S1 in the supplemental material. Constructs for chlamydial transformation were cloned using high-fidelity (HiFi) cloning system from New England BioLabs (NEB). Primers were designed using the NEBuilder online primer generation tool (<https://nebuilder1.neb.com>). For the overexpression strain, the *ahpC* gene was amplified by PCR with Phusion DNA polymerase

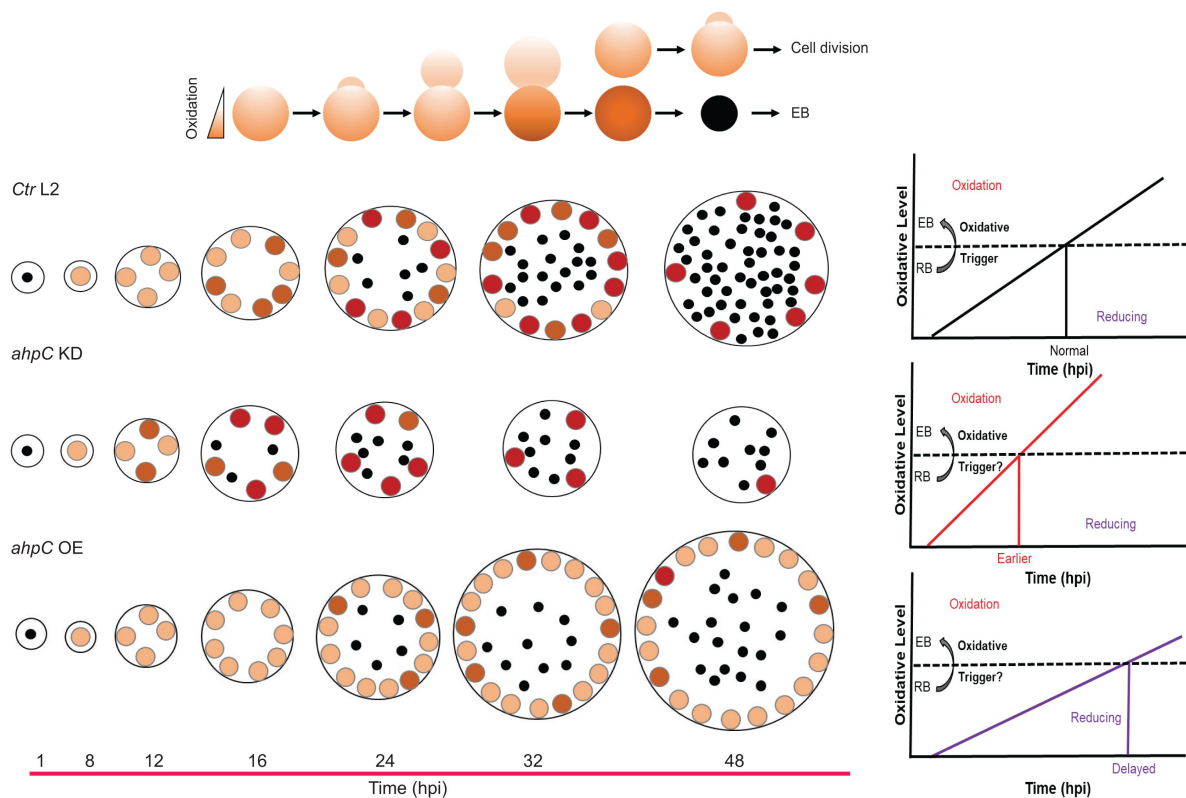


**Fig. 8**

Altering the activity of AhpC in *Ctr* L2 impacts its developmental cycle progression. (Top) In *Chlamydia*, secondary differentiation is asynchronous and RBs divide through an asymmetric budding mechanism. In such conditions, either the mother or daughter cell may inherit more oxidized proteins (represented by a darker shade), which can then impact whether a given RB will divide again or undergo secondary differentiation. (Bottom) The black dots represent EBs, the orange circles show RBs. The developmental cycle of wild-type *C. trachomatis* (Ctr L2) is shown. In *ahpC* KD, highly oxidized conditions lead some RBs to cross the oxidative threshold sooner, allowing activation of late genes and secondary differentiation earlier than other RBs. In *ahpC* overexpression, a reducing environment results in a delay in achieving the oxidative threshold, thus allowing RBs to continue to divide before committing to secondary differentiation.

(NEB) using *C. trachomatis* serovar L2 434/Bu genomic DNA as a template. The PCR product was purified using a PCR purification kit (Qiagen, Hilden, Germany). The HiFi assembly reaction was performed as per the manufacturer's instructions in conjunction with the pBOMBDC plasmid digested with Fast Digest EagI and KpnI enzymes and dephosphorylated with FastAP (Thermo Fisher, Waltham, MA). The HiFi reaction mix was transformed into *E. coli* 10 $\beta$  (NEB). Plasmids were first confirmed by restriction enzyme digestion, and final verification of insert was performed using Sanger sequencing. A dCas12-based CRISPRi approach was used for *ahpC* knockdown generation (Ouellette et al., 2021 [DOI](#)). The pBOMBL12CRia plasmid having anhydrotetracycline (aTc) inducible catalytically dead dCas12 protein was used as vector. A crRNA targeting the 5' intergenic region of *ahpC* was designed and ordered as a presynthesized DNA fragment. For *ahpC* knockdown construct, 2 ng of the gBlock (Integrated DNA Technologies [IDT], Coralville, IA) listed in Table S1 was combined with 25 ng of BamHI-digested, alkaline phosphatase-treated pBOMBL12CRia(e.v.):L2 in a HiFi reaction according to the manufacturer's instructions (NEB). The plasmid was transformed into NEB 10 $\beta$  cells and verified by Sanger sequencing prior to transformation into *Chlamydia trachomatis*. To generate the complementation strain, the *ahpC* gene was amplified using primers listed in Table S1 and fused with the *ahpC* knockdown construct (i.e., pBOMBL12CRia (*ahpC*)) digested with the Fast Digest restriction enzyme Sall (Thermo Fisher) and alkaline phosphatase-treated, using the HiFi reaction as mentioned above.

## Chlamydial transformation

Chlamydial transformations were performed using a protocol described previously, with some modifications (Mueller et al., 2017 [DOI](#)). One day before transformation, 1 x 10<sup>6</sup> McCoy cells were seeded in one 6-well plate, and two wells were used per plasmid transformation. Briefly, for each well of the 6-well plate, 2  $\mu$ g of sequenced verified plasmids were incubated with 2.5 x 10<sup>6</sup> *C. trachomatis* serovar L2 without plasmid (-pL2) EBs in 50  $\mu$ L Tris-CaCl<sub>2</sub> (10 mM Tris, 50 mM CaCl<sub>2</sub>, pH 7.4) at room temperature for 30 min. McCoy cells were washed with 2 mL Hank's Balanced Salt Solution (HBSS; Gibco), and 1 mL HBSS was added back into each well. 1 mL of HBSS was added to each transformant mixture, and one well of a 6-well plate was infected using this transformation solution. Cells were centrifuged at 400  $\times$  g for 15 min at room temperature followed by 15 min incubation at 37°C. HBSS was aspirated and replaced with antibiotic-free DMEM. At 8 hpi, 1  $\mu$ g/mL of cycloheximide and 1 or 2 U/mL of penicillin G or 500  $\mu$ g/mL spectinomycin were added to the culture media. The infection was passaged every 48 h until a population of penicillin or spectinomycin resistant, green fluorescent protein (GFP) positive *C. trachomatis* was established. The chlamydial transformants were then serially diluted to isolate clonal populations. These isolated populations were further expanded and frozen at -80°C in a sucrose phosphate solution (2SP). To verify plasmid sequences, DNA was harvested from infected cultures using the DNeasy kit (Qiagen) and transformed into NEB 10 $\beta$  for plasmid propagation. Isolated plasmids were then verified by restriction digest and Sanger sequencing.

## Inclusion forming unit assay

Inclusion forming unit assay was performed to determine the infectious progeny (number of EBs) from a primary infection based on inclusions formed in a secondary infection. *C. trachomatis* transformants were infected into HeLa cells and induced or not with 1 nM aTc at 10 hpi. At 24 and 48 hpi, samples were harvested by scraping three wells of a 24-well plate in 2 sucrose-phosphate (2SP) solution and lysed via a single freeze-thaw cycle, serially diluted, and used to infect a fresh HeLa cell monolayer and allowed to grow for 24 h. Samples were fixed with methanol, stained with a goat antibody specific to *C. trachomatis* major outer membrane protein (MOMP; Meridian Biosciences, Memphis TN) followed by staining with donkey antigoat Alexa Fluor 594-conjugated secondary antibody (Invitrogen) and titers were enumerated using a 20x lens objective. All experiments were performed three times for three biological replicates. Induced values were expressed as a percentage of the uninduced values, which was considered as 100%.

## Immunofluorescence assay

HeLa cells were cultured on glass coverslips in 24-well tissue culture plates at  $2 \times 10^5$  cells/well, infected with the relevant strains, and, at 10 hpi, samples were induced or not with 1 nM aTc. At 24 hpi, samples were fixed and permeabilized using 100% methanol. Organisms were stained with anti-MOMP (Meridian Biosciences) primary antibody for all the strains and primary mouse anti-Cpf1 (dCas12) (Sigma-Millipore) for knockdown or complementation samples. Donkey anti-goat Alexa Fluor 594-conjugated secondary antibody (Invitrogen) was used to visualize *Chlamydia* in all the samples, and donkey anti-mouse Alexa Fluor 488-conjugated secondary antibody (Invitrogen) was used for dCas12 expression. DAPI (Invitrogen) was used for visualization of host and bacterial cell DNA. These stained coverslips were mounted on glass slides using ProLong glass antifade mounting media (Invitrogen) and imaged using a 100x lens objective on a Zeiss Axioimager Z.2 equipped with Apotome.2 optical sectioning hardware and X-Cite Series 120PC illumination lamp using a 2MP AxioCam 506 monochrome camera.

## Nucleic acid extraction and RT-qPCR

HeLa cells were seeded in 6-well tissue culture plates, infected with the *C. trachomatis* transformants, and induced or not at 10 hpi with 1 nM aTc. For each condition, triplicate wells were used for simultaneous harvest of RNA (for transcript analysis by RT-qPCR), gDNA (to normalize RT-qPCR data and quantification of gDNA), and IFA (to verify the morphological changes in samples in the tested conditions). For RNA extraction, cells were rinsed with DPBS twice and lysed with 1 mL TRIzol (Invitrogen/Thermo Fisher) per well as per manufacturer's instructions. 200  $\mu$ L of chloroform was added to extract the aqueous layer containing total RNA, which was precipitated with isopropanol. A total of 10  $\mu$ g of purified RNA was treated with TURBO DNase (Invitrogen/Thermo Fisher) according to the manufacturer's instructions to remove DNA contamination. DNA-free RNA was used for cDNA synthesis using random nonamers (N9; NEB) and SuperScript III reverse transcriptase (Invitrogen/Thermo Fisher) following the manufacturer's instructions. cDNA samples were diluted 10-fold with molecular biology-grade water and stored at  $-80^{\circ}\text{C}$ . A total of 2.5  $\mu$ L of each diluted cDNA sample was used per well of a 96-well qPCR plate. For each of three biological replicates, each sample was analyzed in triplicate on a QuantStudio 3 system (Applied Biosystems/Thermo Fisher) using the standard amplification cycle with melting curve analysis. For gDNA, one well of a 6-well plate per condition was scraped in 500  $\mu$ L DPBS, split in half (i.e., 250  $\mu$ L), and frozen at  $-80^{\circ}\text{C}$ . Each sample was then thawed and frozen twice more for a total of three freeze/thaw cycles, and gDNA was extracted using the DNeasy DNA extraction kit (Qiagen) according to the manufacturer's guidelines. The isolated gDNA was quantified and diluted down to 5 ng/mL prior to use in quantitative PCR (qPCR). A total of 2.5  $\mu$ L of each diluted gDNA sample was mixed with 10  $\mu$ L of PowerUp SYBR green master mix in a 96-well qPCR plate and was analyzed on a QuantStudio 3 system (Applied Biosystems). Each sample from each biological replicate was tested in triplicate. For each primer set used, a standard curve of gDNA was generated against purified *C. trachomatis* L2 genomic DNA, and the cDNA levels were normalized to gDNA levels or 16S rRNA for analysis. All experiments were performed three times for three biological replicates. At the same time, morphological differences were monitored in the IFA control, with samples fixed with methanol at the time of harvesting of RNA/gDNA. Staining and imaging were performed as described above.

## Viability assay

Cell viability assays were performed using PrestoBlue (Invitrogen/Thermo Fisher). HeLa cells were seeded in 96 well plates and were infected or not with the indicated chlamydial strains (e.g., pBOMBDC.ev). Samples were treated or not as per the experimental parameters (e.g., different concentrations of oxidizing agents or scavengers). Medium without cells was used as the blank control. At the end point, 10% PrestoBlue (v/v) was added in the wells and incubated at  $37^{\circ}\text{C}$  for 30 min while protecting the plate from light. Fluorescence was read at excitation 560 nm and

emission 590 nm using an Infinite M200 Pro (Tecan). The treated values were expressed as a percentage of the untreated values, which was considered as 100%. All experiments were performed three times for three biological replicates.

## Oxidizing agents' susceptibility testing

Susceptibility of host cells and chlamydiae to different oxidizing agents was tested in HeLa cells infected with density gradient-purified *Chlamydia trachomatis* 434/Bu EBs or *C. trachomatis* transformants. For *C. trachomatis* transformants, expression of the construct was induced or not with 1 nM aTc at 10 hpi. At 16 hpi, different concentrations of oxidizing agents were added, and samples were incubated at 37°C for 30 min. These samples were washed three times with HBSS, fresh DMEM media was added in the wells, and cultures were allowed to grow until 24 hpi. At 24 hpi, inclusion forming unit assays and immunofluorescence analysis were performed as described above.

## ROS scavenging by chemical compounds

The scavenging capacity of different ROS scavengers was tested using HeLa cells infected with *Chlamydia trachomatis* 434/Bu EBs or the *ahpC* KD strain. To examine the protective effect of scavengers in the absence or presence of oxidative stress, *Chlamydia trachomatis* 434/Bu EBs infected HeLa cells were used. In these samples, scavengers were added or not at 10 hpi in respective wells. At 16 hpi, wells were washed three times with HBSS, and fresh DMEM containing 500 µM H<sub>2</sub>O<sub>2</sub> or not was added. After 30 min, wells were washed three times with HBSS and fresh DMEM containing scavengers or not was added back in the respective wells, which were incubated until 24 hpi prior to collecting samples for IFU assay and IFA analysis. The effect of these scavengers was further tested in *ahpC* KD. HeLa cells were infected with *ahpC* KD, scavengers were added or not at 9.5 hpi before induction at 10 hpi with 1nM aTc. At 14 hpi, scavengers were added again in the respective wells, and, at 24 hpi, samples were collected for IFU assay and IFA.

## ROS detection by CellROX Deep Red

Intracellular ROS levels were measured in uninfected and *ahpC* KD-infected HeLa cells using CellROX Deep Red dye (Invitrogen/Thermo Fisher). Samples were induced or not at 10 hpi with 1 nM aTc. Medium without cells was used as the blank control. At 16 hpi, samples were treated or not with 62.5 µM or 1 mM TBHP for 30 min. At the end point, media was removed, samples were washed three times with DPBS and incubated with CellROX Deep Red dye for 30 min in the dark at 37°C. Fluorescence was read at excitation 644 nm and emission 665 nm using an Infinite M200 Pro (Tecan). All experiments were performed three times for three biological replicates.

## Acknowledgements

We thank Dr. H. Caldwell (NIH/NIAID) for providing eukaryotic cell lines and Dr. I. Clarke (University of Southampton) for providing the plasmid less strain of *C. trachomatis* serovar L2. We thank Dr. Elizabeth A. Rucks for critical feedback. We thank the members of the Rucks/Ouellette research group for thoughtful discussion of the material presented. Funding for this work was provided by the National Institutes of Health (NIH/NIAID) grants R01AI170688 and R21AI178150 to SPO.

## Supplementary Information

**Table S1** List of plasmids, strains, and primers used in this study.

**Fig. S1** Viability assay of uninfected or infected HeLa cells treated with oxidizing agents  $H_2O_2$  (A), CHP (B), TBHP (C), and PN (D). HeLa cells were infected or not with empty vector control, pBOMBDC.ev (EV), and treated or not with different concentrations of oxidizing agents at 16 hpi for 30 min. At 24 hpi, an end point viability assay was performed using PrestoBlue as mentioned in materials and methods. The treated values were expressed as a percentage of the untreated values, which were considered as 100%. Data represent three biological replicates.

**Fig. S2** Response of *C. trachomatis* L2 against oxidizing agents. (A) IFA of wild-type *Ctr* L2 exposed to oxidizing agents. Oxidizing agents' treatment, staining, and imaging were performed as mentioned in materials and methods. Representative images from three biological replicates are shown. (B) IFU analysis of *Ctr* L2 post-exposure with oxidizing agents. Conditions were same as in section (A), and IFUs were harvested at 24 hpi. IFUs were calculated as percentage of untreated samples. \*\*\* $p < 0.0001$  vs untreated sample by using one way ANOVA. Data represent three biological replicates.

**Fig. S3** Overexpression of *ahpC* provides resistance to peroxides in *Chlamydia*. IFA of *ahpC* (A) or EV (B) exposed to oxidizing agents (CHP, TBHP, and PN). Experiments were performed as mentioned in the legend of **Fig. 3A**. Representative images from three biological replicates are shown.

**Fig. S4** *Chlamydia* is hypersensitive to oxidizing agents as a result of reduced levels of *ahpC*. IFA of *ahpC* KD (A), NT (B), comp (C) treated with CHP, TBHP, and PN. Experimental conditions were the same as mentioned in the legend of **Fig. 5A**. Representative images from three biological replicates are shown.

**Fig. S5** Rescue of oxidative stress phenotype by ROS scavengers in *C. trachomatis* L2. (A) IFA of wild-type *Ctr* L2 incubated or not with scavengers,  $\alpha$ -Tocopherol (100  $\mu$ M) and DMTU (10 mM), and treated or not with 500  $\mu$ M  $H_2O_2$  as mentioned in materials and methods. Representative images from three biological replicates are shown. (B) IFU analysis of *Ctr* L2 grown under the same conditions as mentioned in the legend of **Fig. 6G**. IFUs were calculated as percentage of untreated samples. \*\*\* $p < 0.0001$ , statistical analysis was performed using ordinary one-way ANOVA.  $H_2O_2$  treated sample and samples incubated with scavengers only were compared to the untreated control. Samples treated with  $H_2O_2$  and incubated with scavengers were compared with sample treated with  $H_2O_2$ . Data represent three biological replicates. Only significant differences are noted.

**Fig. S6** Effect of penicillin treatment during *ahpC* knockdown. (A) IFA was performed to assess inclusion size and morphology of *ahpC* KD-spec following induction (1 nM aTc) and penicillin treatment (1 U/mL) at 10 hpi. At 24 hpi, cells were fixed with methanol and stained using primary antibodies to major outer membrane protein (MOMP), Cpf1 (dCas12), and DAPI. All images were acquired on Zeiss Axio Imager Z.2 with Apotome2 at 100x magnification. Bars, 2  $\mu$ m. Representative images of three biological replicates are shown. Transcriptional analysis of (B) *ahpC*, (C) *hctA*, and (D) *hctB* in *ahpC* KD-spec using RT-qPCR using the same conditions as in section (A). RNA samples were harvested at 16 and 24 hpi. Quantified cDNA was normalized to 16SrRNA, and values were plotted on a log scale. \*\*\* $p < 0.0001$ , \*\* $p < 0.001$ , \* $p < 0.01$  vs uninduced sample by using two-way ANOVA. Data represent three biological replicates.

## References

- Abdelrahman Y., Ouellette S. P., Belland R. J., Cox J. V. (2016) **Polarized Cell Division of *Chlamydia trachomatis*** *PLoS Pathog* **12** <https://doi.org/10.1371/journal.ppat.1005822>
- Abdelrahman Y. M., Belland R. J. (2005) **The chlamydial developmental cycle** *FEMS Microbiol Rev* **29**:949–959 <https://doi.org/10.1016/j.femsre.2005.03.002>
- Abdul-Sater A. A. *et al.* (2010) **Enhancement of reactive oxygen species production and chlamydial infection by the mitochondrial Nod-like family member NLRX1** *J Biol Chem* **285**:41637–41645 <https://doi.org/10.1074/jbc.M110.137885>
- Antelmann H., Engelmann S., Schmid R., Hecker M. (1996) **General and oxidative stress responses in *Bacillus subtilis*: cloning, expression, and mutation of the alkyl hydroperoxide reductase operon** *J Bacteriol* **178**:6571–6578 <https://doi.org/10.1128/jb.178.22.6571-6578.1996>
- Barbour A. G., Amano K., Hackstadt T., Perry L., Caldwell H. D. (1982) ***Chlamydia trachomatis* has penicillin-binding proteins but not detectable muramic acid** *J Bacteriol* **151**:420–428 <https://doi.org/10.1128/jb.151.1.420-428.1982>
- Belland R. J., Zhong G., Crane D. D., Hogan D., Sturdevant D., Sharma J., Beatty W. L., Caldwell H. D. (2003) **Genomic transcriptional profiling of the developmental cycle of *Chlamydia trachomatis*** *Proc Natl Acad Sci U S A* **100**:8478–8483 <https://doi.org/10.1073/pnas.1331135100>
- Betts-Hampikian H. J., Fields K. A. (2011) **Disulfide bonding within components of the *Chlamydia* type III secretion apparatus correlates with development** *J Bacteriol* **193**:6950–6959 <https://doi.org/10.1128/JB.05163-11>
- Boncompain G., Muller C., Meas-Yedid V., Schmitt-Kopplin P., Lazarow P. B., Subtil A. (2014) **The intracellular bacteria *Chlamydia* hijack peroxisomes and utilize their enzymatic capacity to produce bacteria-specific phospholipids** *PLoS One* **9** <https://doi.org/10.1371/journal.pone.0086196>
- Boncompain G., Schneider B., Delevoye C., Kellermann O., Dautry-Varsat A., Subtil A. (2010) **Production of reactive oxygen species is turned on and rapidly shut down in epithelial cells infected with *Chlamydia trachomatis*** *Infect Immun* **78**:80–87 <https://doi.org/10.1128/IAI.00725-09>
- Brinkworth A. J., Wildung M. R., Carabeo R. A. (2018) **Genomewide Transcriptional Responses of Iron-Starved *Chlamydia trachomatis* Reveal Prioritization of Metabolic Precursor Synthesis over Protein Translation** *mSystems* **3** <https://doi.org/10.1128/mSystems.00184-17>
- Caldwell H. D., Kromhout J., Schachter J. (1981) **Purification and partial characterization of the major outer membrane protein of *Chlamydia trachomatis*** *Infect Immun* **31**:1161–1176 <https://doi.org/10.1128/iai.31.3.1161-1176.1981>
- Chiarelli T. J., Grieshaber N. A., Omsland A., Remien C. H., Grieshaber S. S. (2020) **Single-Inclusion Kinetics of *Chlamydia trachomatis* Development** *mSystems* **5** <https://doi.org/10.1128/mSystems.00689-20>

- Clifton D. R., Dooley C. A., Grieshaber S. S., Carabeo R. A., Fields K. A., Hackstadt T. (2005) **Tyrosine phosphorylation of the chlamydial effector protein Tarp is species specific and not required for recruitment of actin** *Infect Immun* **73**:3860–3868 <https://doi.org/10.1128/IAI.73.7.3860-3868.2005>
- Cosgrove K., Coutts G., Jonsson I. M., Tarkowski A., Kokai-Kun J. F., Mond J. J., Foster S. J. (2007) **Catalase (KatA) and alkyl hydroperoxide reductase (AhpC) have compensatory roles in peroxide stress resistance and are required for survival, persistence, and nasal colonization in Staphylococcus aureus** *J Bacteriol* **189**:1025–1035 <https://doi.org/10.1128/JB.01524-06>
- Cox J. V., Abdelrahman Y. M., Ouellette S. P. (2020) **Penicillin-binding proteins regulate multiple steps in the polarized cell division process of Chlamydia** *Sci Rep* **10** <https://doi.org/10.1038/s41598-020-69397-x>
- de Oliveira M. A., Tairum C. A., Netto L. E. S., de Oliveira A. L. P., Aleixo-Silva R. L., Cabrera V. I. M., Breyer C. A., Dos Santos M. C. (2021) **Relevance of peroxiredoxins in pathogenic microorganisms** *Appl Microbiol Biotechnol* **105**:5701–5717 <https://doi.org/10.1007/s00253-021-11360-5>
- Dip P. V. *et al.* (2014) **Key roles of the Escherichia coli AhpC C-terminus in assembly and catalysis of alkylhydroperoxide reductase, an enzyme essential for the alleviation of oxidative stress** *Biochim Biophys Acta* **1837**:1932–1943 <https://doi.org/10.1016/j.bbambio.2014.08.007>
- Everett K. D., Hatch T. P. (1995) **Architecture of the cell envelope of Chlamydia psittaci 6BC** *J Bacteriol* **177**:877–882 <https://doi.org/10.1128/jb.177.4.877-882.1995>
- Ezraty B., Gennaris A., Barras F., Collet J. F. (2017) **Oxidative stress, protein damage and repair in bacteria** *Nat Rev Microbiol* **15**:385–396 <https://doi.org/10.1038/nrmicro.2017.26>
- Fang F. C. (2011) **Antimicrobial actions of reactive oxygen species** *mBio* **2** <https://doi.org/10.1128/mBio.00141-11>
- Feng X., Guo K., Gao H. (2020) **Plasticity of the peroxidase AhpC links multiple substrates to diverse disulfide-reducing pathways in Shewanella oneidensis** *J Biol Chem* **295**:11118–11130 <https://doi.org/10.1074/jbc.RA120.014010>
- Gehre L., Gorgette O., Perrinet S., Prevost M. C., Ducatez M., Giebel A. M., Nelson D. E., Ball S. G., Subtil A. (2016) **Sequestration of host metabolism by an intracellular pathogen** *Elife* **5** <https://doi.org/10.7554/eLife.12552>
- Gerard H. C. *et al.* (2002) **Chlamydia trachomatis genes whose products are related to energy metabolism are expressed differentially in active vs. persistent infection** *Microbes Infect* **4**:13–22 [https://doi.org/10.1016/s1286-4579\(01\)01504-0](https://doi.org/10.1016/s1286-4579(01)01504-0)
- Hatch N. D., Ouellette S. P. (2023) **Identification of the alternative sigma factor regulons of Chlamydia trachomatis using multiplexed CRISPR interference** *mSphere* **8** <https://doi.org/10.1128/msphere.00391-23>
- Hollander-Czytko H., Grabowski J., Sandorf I., Weckermann K., Weiler E. W. (2005) **Tocopherol content and activities of tyrosine aminotransferase and cystine lyase in Arabidopsis under stress conditions** *J Plant Physiol* **162**:767–770 <https://doi.org/10.1016/j.jplph.2005.04.019>

- Iliffe-Lee E. R., McClarty G. (1999) **Glucose metabolism in Chlamydia trachomatis: the 'energy parasite' hypothesis revisited** *Mol Microbiol* **33**:177–187 <https://doi.org/10.1046/j.1365-2958.1999.01464.x>
- Kiffin R., Bandyopadhyay U., Cuervo A. M. (2006) **Oxidative stress and autophagy** *Antioxid Redox Signal* **8**:152–162 <https://doi.org/10.1089/ars.2006.8.152>
- Kimura A., Yuhara S., Ohtsubo Y., Nagata Y., Tsuda M. (2012) **Suppression of pleiotropic phenotypes of a Burkholderia multivorans fur mutant by oxyR mutation** *Microbiology (Reading)* **158**:1284–1293 <https://doi.org/10.1099/mic.0.057372-0>
- Koshkin A., Knudsen G. M., De Montellano Ortiz, P. R (2004) **Intermolecular interactions in the AhpC/AhpD antioxidant defense system of Mycobacterium tuberculosis** *Arch Biochem Biophys* **427**:41–47 <https://doi.org/10.1016/j.abb.2004.04.017>
- Lee J., Cox J. V., Ouellette S. P. (2020) **Critical Role for the Extended N Terminus of Chlamydial MreB in Directing Its Membrane Association and Potential Interaction with Divisome Proteins** *J Bacteriol* **202** <https://doi.org/10.1128/JB.00034-20>
- Loprasert S., Sallabhan R., Whangsuk W., Mongkolsuk S. (2003) **Compensatory increase in ahpC gene expression and its role in protecting Burkholderia pseudomallei against reactive nitrogen intermediates** *Arch Microbiol* **180**:498–502 <https://doi.org/10.1007/s00203-003-0621-9>
- Mastronicola D., Falabella M., Testa F., Pucillo L. P., Teixeira M., Sarti P., Saraiva L. M., Giuffrè A. (2014) **Functional characterization of peroxiredoxins from the human protozoan parasite Giardia intestinalis** *PLoS Negl Trop Dis* **8** <https://doi.org/10.1371/journal.pntd.0002631>
- Matsumoto A., Manire G. P. (1970) **Electron Microscopic Observations on the Fine Structure of Cell Walls of Chlamydia psittaci** *J Bacteriol* **104**:1332–1337 <https://doi.org/10.1128/jb.104.3.1332-1337.1970>
- Mishra S., Imlay J. (2012) **Why do bacteria use so many enzymes to scavenge hydrogen peroxide?** *Arch Biochem Biophys* **525**:145–160 <https://doi.org/10.1016/j.abb.2012.04.014>
- Mongkolsuk S., Whangsuk W., Vattanaviboon P., Loprasert S., Fuangthong M. (2000) **A Xanthomonas alkyl hydroperoxide reductase subunit C (ahpC) mutant showed an altered peroxide stress response and complex regulation of the compensatory response of peroxide detoxification enzymes** *J Bacteriol* **182**:6845–6849 <https://doi.org/10.1128/JB.182.23.6845-6849.2000>
- Moulder J. W. (1993) **Why is Chlamydia sensitive to penicillin in the absence of peptidoglycan?** *Infect Agents Dis* **2**:87–99
- Moulder J. W., Colon J. I., Ruda J., Zebrovitz M. M. (1956) **The effect of penicillin on multiplying and nonmultiplying populations of sensitive and resistant strains of feline pneumonitis virus** *J Infect Dis* **98**:229–238 <https://doi.org/10.1093/infdis/98.3.229>
- Mueller K. E., Wolf K., Fields K. A. (2017) **Chlamydia trachomatis Transformation and Allelic Exchange Mutagenesis** *Curr Protoc Microbiol* **45**:11–11 <https://doi.org/10.1002/cpmc.31>
- Mygind P., Christiansen G., Persson K., Birkelund S. (1998) **Analysis of the humoral immune response to Chlamydia outer membrane protein 2** *Clin Diagn Lab Immunol* **5**:313–318 <https://doi.org/10.1128/CDLI.5.3.313-318.1998>

- Newhall W. J. t. (1987) **Biosynthesis and disulfide cross-linking of outer membrane components during the growth cycle of *Chlamydia trachomatis*** *Infect Immun* **55**:162–168 <https://doi.org/10.1128/iai.55.1.162-168.1987>
- Ochsner U. A., Vasil M. L., Alsabbagh E., Parvatiyar K., Hassett D. J. (2000) **Role of the *Pseudomonas aeruginosa* oxyR-recG operon in oxidative stress defense and DNA repair: OxyR-dependent regulation of katB-ankB, ahpB, and ahpC-ahpF** *J Bacteriol* **182**:4533–4544 <https://doi.org/10.1128/JB.182.16.4533-4544.2000>
- Oh E., Jeon B. (2014) **Role of alkyl hydroperoxide reductase (AhpC) in the biofilm formation of *Campylobacter jejuni*** *PLoS One* **9** <https://doi.org/10.1371/journal.pone.0087312>
- Ouellette S. P. (2018) **Feasibility of a Conditional Knockout System for *Chlamydia* Based on CRISPR Interference** *Front Cell Infect Microbiol* **8** <https://doi.org/10.3389/fcimb.2018.00059>
- Ouellette S. P., Blay E. A., Hatch N. D., Fisher-Marvin L. A. (2021) **CRISPR Interference To Inducibly Repress Gene Expression in *Chlamydia trachomatis*** *Infect Immun* **89** <https://doi.org/10.1128/IAI.00108-21>
- Ouellette S. P., Fisher-Marvin L. A., Harpring M., Lee J., Rucks E. A., Cox J. V. (2022) **Localized cardiolipin synthesis is required for the assembly of MreB during the polarized cell division of *Chlamydia trachomatis*** *PLoS Pathog* **18** <https://doi.org/10.1371/journal.ppat.1010836>
- Ouellette S. P., Hatch T. P., AbdelRahman Y. M., Rose L. A., Belland R. J., Byrne G. I. (2006) **Global transcriptional upregulation in the absence of increased translation in *Chlamydia* during IFN $\gamma$ -mediated host cell tryptophan starvation** *Mol Microbiol* **62**:1387–1401 <https://doi.org/10.1111/j.1365-2958.2006.05465.x>
- Ouellette S. P., Karimova G., Subtil A., Ladant D. (2012) ***Chlamydia* co-opts the rod shape-determining proteins MreB and Pbp2 for cell division** *Mol Microbiol* **85**:164–178 <https://doi.org/10.1111/j.1365-2958.2012.08100.x>
- Ouellette S. P., Lee J., Cox J. V. (2020) **Division without Binary Fission: Cell Division in the FtsZ-Less *Chlamydia*** *J Bacteriol* **202** <https://doi.org/10.1128/JB.00252-20>
- Pan S., Jensen A. A., Wood N. A., Henrichfreise B., Brotz-Oesterhelt H., Fisher D. J., Sass P., Ouellette S. P. (2023) **Molecular Characterization of the ClpC AAA+ ATPase in the Biology of *Chlamydia trachomatis*** *mBio* **14** <https://doi.org/10.1128/mbio.00075-23>
- Panzetta M. E., Valdivia R. H., Saka H. A. (2018) ***Chlamydia* Persistence: A Survival Strategy to Evade Antimicrobial Effects in-vitro and in-vivo** *Front Microbiol* **9** <https://doi.org/10.3389/fmicb.2018.03101>
- Parsonage D., Karplus P. A., Poole L. B. (2008) **Substrate specificity and redox potential of AhpC, a bacterial peroxiredoxin** *Proc Natl Acad Sci U S A* **105**:8209–8214 <https://doi.org/10.1073/pnas.0708308105>
- Pokorzynski N. D., Brinkworth A. J., Carabeo R. (2019) **A bipartite iron-dependent transcriptional regulation of the tryptophan salvage pathway in *Chlamydia trachomatis*** *Elife* **8** <https://doi.org/10.7554/eLife.42295>

- Poole L. B., Ellis H. R. (1996) **Flavin-dependent alkyl hydroperoxide reductase from *Salmonella typhimurium*. 1. Purification and enzymatic activities of overexpressed AhpF and AhpC proteins** *Biochemistry* **35**:56–64 <https://doi.org/10.1021/bi951887s>
- Reuter J. *et al.* (2023) **An NlpC/P60 protein catalyzes a key step in peptidoglycan recycling at the intersection of energy recovery, cell division and immune evasion in the intracellular pathogen *Chlamydia trachomatis*** *PLoS Pathog* **19** <https://doi.org/10.1371/journal.ppat.1011047>
- Richard D., Bartfai R., Volz J., Ralph S. A., Muller S., Stunnenberg H. G., Cowman A. F. (2011) **A genome-wide chromatin-associated nuclear peroxiredoxin from the malaria parasite *Plasmodium falciparum*** *J Biol Chem* **286**:11746–11755 <https://doi.org/10.1074/jbc.M110.198499>
- Rusconi B., Greub G. (2013) **Discovery of catalases in members of the Chlamydiales order** *J Bacteriol* **195**:3543–3551 <https://doi.org/10.1128/JB.00563-13>
- Seaver L. C., Imlay J. A. (2001) **Alkyl hydroperoxide reductase is the primary scavenger of endogenous hydrogen peroxide in *Escherichia coli*** *J Bacteriol* **183**:7173–7181 <https://doi.org/10.1128/JB.183.24.7173-7181.2001>
- Sherman D. R., Mdluli K., Hickey M. J., Barry C. E., Stover C. K. (1999) **AhpC, oxidative stress and drug resistance in *Mycobacterium tuberculosis*** *Biofactors* **10**:211–217 <https://doi.org/10.1002/biof.5520100219>
- Soules K. R., Dmitriev A., LaBrie S. D., Dimond Z. E., May B. H., Johnson D. K., Zhang Y., Battaile K. P., Lovell S., Hefty P. S. (2020) **Structural and ligand binding analyses of the periplasmic sensor domain of RsbU in *Chlamydia trachomatis* support a role in TCA cycle regulation** *Mol Microbiol* **113**:68–88 <https://doi.org/10.1111/mmi.14401>
- Soules K. R., LaBrie S. D., May B. H., Hefty P. S. (2020) **Sigma 54-Regulated Transcription Is Associated with Membrane Reorganization and Type III Secretion Effectors during Conversion to Infectious Forms of *Chlamydia trachomatis*** *mBio* **11** <https://doi.org/10.1128/mBio.01725-20>
- Staerck C., Gastebois A., Vandeputte P., Calenda A., Larcher G., Gillmann L., Papon N., Bouchara J. P., Fleury M. J. J. (2017) **Microbial antioxidant defense enzymes** *Microb Pathog* **110**:56–65 <https://doi.org/10.1016/j.micpath.2017.06.015>
- Storz G., Jacobson F. S., Tartaglia L. A., Morgan R. W., Silveira L. A., Ames B. N. (1989) **An alkyl hydroperoxide reductase induced by oxidative stress in *Salmonella typhimurium* and *Escherichia coli*: genetic characterization and cloning of *ahp*** *J Bacteriol* **171**:2049–2055 <https://doi.org/10.1128/jb.171.4.2049-2055.1989>
- Sun Z., Sun Y., Li Y., Luan X., Chen H., Wu H., Peng B., Lu C. (2020) **Identification of HeLa cell proteins that interact with *Chlamydia trachomatis* glycogen synthase using yeast two-hybrid assays** *Mol Med Rep* **21**:1572–1580 <https://doi.org/10.3892/mmr.2020.10947>
- Swoboda A. R., Wood N. A., Saery E. A., Fisher D. J., Ouellette S. P. (2023) **The Periplasmic Tail-Specific Protease, Tsp, Is Essential for Secondary Differentiation in *Chlamydia trachomatis*** *J Bacteriol* **205** <https://doi.org/10.1128/jb.00099-23>

- Thompson C. C., Griffiths C., Nicod S. S., Lowden N. M., Wigneshweraraj S., Fisher D. J., McClure M. O. (2015) **The Rsb Phosphoregulatory Network Controls Availability of the Primary Sigma Factor in Chlamydia trachomatis and Influences the Kinetics of Growth and Development** *PLoS Pathog* **11** <https://doi.org/10.1371/journal.ppat.1005125>
- Walch M., Dotiwala F., Mulik S., Thiery J., Kirchhausen T., Clayberger C., Krensky A. M., Martinvalet D., Lieberman J. (2015) **Cytotoxic Cells Kill Intracellular Bacteria through Granulysin-Mediated Delivery of Granzymes** *Cell* **161** <https://doi.org/10.1016/j.cell.2015.05.021>
- Wan F., Feng X., Yin J., Gao H. (2021) **Distinct H(2)O(2)-Scavenging System in Yersinia pseudotuberculosis: KatG and AhpC Act Together to Scavenge Endogenous Hydrogen Peroxide** *Front Microbiol* **12** <https://doi.org/10.3389/fmicb.2021.626874>
- Wang G., Conover R. C., Benoit S., Olczak A. A., Olson J. W., Johnson M. K., Maier R. J. (2004) **Role of a bacterial organic hydroperoxide detoxification system in preventing catalase inactivation** *J Biol Chem* **279**:51908–51914 <https://doi.org/10.1074/jbc.M408450200>
- Wang X., Schwarzer C., Hybiske K., Machen T. E., Stephens R. S. (2014) **Developmental stage oxidoreductive states of Chlamydia and infected host cells** *mBio* **5** <https://doi.org/10.1128/mBio.01924-14>
- Wang Y., Kahane S., Cutcliffe L. T., Skilton R. J., Lambden P. R., Clarke I. N. (2011) **Development of a transformation system for Chlamydia trachomatis: restoration of glycogen biosynthesis by acquisition of a plasmid shuttle vector** *PLoS Pathog* **7** <https://doi.org/10.1371/journal.ppat.1002258>
- Wong C. F., Shin J., Subramanian Manimekalai M. S., Saw W. G., Yin Z., Bhushan S., Kumar A., Ragunathan P., Grüber G. (2017) **AhpC of the mycobacterial antioxidant defense system and its interaction with its reducing partner Thioredoxin-C** *Sci Rep* **7** <https://doi.org/10.1038/s41598-017-05354-5>
- Wood N. A., Swoboda A. R., Blocker A. M., Fisher D. J., Ouellette S. P. (2022) **Tag-Dependent Substrate Selection of ClpX Underlies Secondary Differentiation of Chlamydia trachomatis** *mBio* **13** <https://doi.org/10.1128/mbio.01858-22>
- Yang K. S., Kang S. W., Woo H. A., Hwang S. C., Chae H. Z., Kim K., Rhee S. G. (2002) **Inactivation of human peroxiredoxin I during catalysis as the result of the oxidation of the catalytic site cysteine to cysteine-sulfinic acid** *J Biol Chem* **277**:38029–38036 <https://doi.org/10.1074/jbc.M206626200>
- Zhang B., Gu H., Yang Y., Bai H., Zhao C., Si M., Su T., Shen X. (2019) **Molecular Mechanisms of AhpC in Resistance to Oxidative Stress in Burkholderia thailandensis** *Front Microbiol* **10** <https://doi.org/10.3389/fmicb.2019.01483>
- Zuo F., Yu R., Khaskheli G. B., Ma H., Chen L., Zeng Z., Mao A., Chen S. (2014) **Homologous overexpression of alkyl hydroperoxide reductase subunit C (ahpC) protects Bifidobacterium longum strain NCC2705 from oxidative stress** *Res Microbiol* **165**:581–589 <https://doi.org/10.1016/j.resmic.2014.05.040>

## Editors

Reviewing Editor

**Bavesh Kana**

University of the Witwatersrand, Johannesburg, South Africa

Senior Editor

**Bavesh Kana**

University of the Witwatersrand, Johannesburg, South Africa

### Reviewer #1 (Public Review):

Summary:

*Chlamydia* spp. has a biphasic developmental cycle consisting of an extracellular, infectious form called an elementary body (EB) and an intracellular, replicative form known as a reticular body (RB). The structural stability of EBs is maintained by extensive cross-linking of outer membrane proteins while the outer membrane proteins of RBs are in a reduced state. The overall redox state of EBs is more oxidized than RBs. The authors propose that the redox state may be a controlling factor in the developmental cycle. To test this, alkyl hydroperoxide reductase subunit C (ahpC) was overexpressed or knocked down to examine effects on developmental gene expression. KD of ahpC induced increased expression of EB-specific genes and accelerated EB production. Conversely, overexpression of ahpC delayed differentiation to EBs. The results suggest that chlamydial redox state may play a role in differentiation.

Strengths:

Uses modern genetic tools to explore the difficult area of temporal gene expression throughout the chlamydial developmental cycle.

Weaknesses:

The environmental signals triggering ahpC expression/activity are not determined.

<https://doi.org/10.7554/eLife.98409.1.sa2>

### Reviewer #2 (Public Review):

The factors that influence the differentiation of EBs and RBs during Chlamydial development are not clearly understood. A previous study had shown a redox oscillation during the Chlamydial developmental cycle. Based on this observation, the authors hypothesize that the bacterial redox state may play a role in regulating the differentiation in Chlamydia. To test their hypothesis, they make knock-down and overexpression strains of the major ROS regulator, ahpC. They show that the knock-down of ahpC leads to a significant increase in ROS levels leading to an increase in the production of elementary bodies and overexpression leads to a decrease in EB production likely caused by a decrease in oxidation. From their observations, they present an interesting model wherein an increase in oxidation favors the production of EBs.

Major concern:

In the absence of proper redox potential measurements, it is not clear if what they observe is a general oxidative stress response, especially when the knock-down of ahpC leads to a significant increase in ROS levels. Direct redox potential measurement in the ahpC

overexpression and knock-down cells is required to support the model. This can be done using the roGFP-based measurements mentioned in the Wang et al. 2014 study cited by the authors.

<https://doi.org/10.7554/eLife.98409.1.sa1>

### Reviewer #3 (Public Review):

#### Summary:

The study reports clearly on the role of the AhpC protein as an antioxidant factor in *Chlamydia trachomatis* and speculates on the role of AhpC as an indirect regulator of developmental transcription induced by redox stress in this differentiating obligate intracellular bacterium.

#### Strengths:

The question posed and the concluding model about redox-dependent differentiation in chlamydia is interesting and highly relevant. This work fits with other propositions in which redox changes have been reported during bacterial developmental cycles, potentially as triggers, but have not been cited (examples PMID: 2865432, PMID: 32090198, PMID: 26063575). Here, AhpC over-expression is shown to protect *Chlamydia* towards redox stress imposed by H<sub>2</sub>O<sub>2</sub>, CHP, TBHP, and PN, while CRISPRi-mediated depletion of AhpC curbed intracellular replication and resulted in increased ROS levels and sensitivity to oxidizing agents. Importantly, the addition of ROS scavengers mitigated the growth defect caused by AhpC depletion. These results clearly establish the role of AhpC affects the redox state and growth in Ct (with the complicated KO genetics and complementation that are very nicely done).

#### Weaknesses:

However, with respect to the most important implication and claims of this work, the role of redox in controlling the chlamydial developmental cycle rather than simply being a correlation/passenger effect, I am less convinced about the impact of this work. First, the study is largely observational and does not resolve how this redox control of the cell cycle could be achieved, whereas in the case of *Caulobacter*, a clear molecular link between DNA replication and redox has been proposed. How would progressive oxidation in RBs eventually trigger the secondary developmental genes to induce EB differentiation? Is there an OxyR homolog that could elicit this change and why would the oxidation stress in RBs gradually accumulate during growth despite the presence of AhpC? In other words, the role of AhpC is simply to delay or dampen the redox stress response until the trigger kicks in, again, what is the trigger? Is this caused by increasing oxidative respiration of RBs in the inclusion? But what determines the redox threshold?

I also find the experiment with Pen treatment to have little predictive power. The fact that transcription just proceeds when division is blocked is not unprecedented. This also happens during the *Caulobacter* cell cycle when FtsZ is depleted for most developmental genes, except for those that are activated upon completion of the asymmetric cell division and that is dependent on the completion of compartmentalization. This is a smaller subset of developmental genes in *caulobacter*, but if there is a similar subset that depends on division on *chlamydia* and if these are affected by redox as well, then the argument about the interplay between developmental transcription and redox becomes much stronger and the link more intriguing. Another possibility to strengthen the study is to show that redox-regulated genes are under the direct control of chlamydial developmental regulators such as

Euo, HctA, or others and at least show dual regulation by these inputs -perhaps the feed occurs through the same path.

This redox-transcription shortcoming is also reflected in the discussion where most are about the effects and molecular mitigation of redox stress in various systems, but there is little discussion on its link with developmental transcription in bacteria in general and chlamydia.

<https://doi.org/10.7554/eLife.98409.1.sa0>